

See discussions, stats, and author profiles for this publication at: <https://www.researchgate.net/publication/5768025>

Lattice model of equilibrium polymerization. VI. Measures of fluid "complexity" and search for generalized corresponding states

ARTICLE *in* THE JOURNAL OF CHEMICAL PHYSICS · JANUARY 2008

Impact Factor: 2.95 · DOI: 10.1063/1.2785187 · Source: PubMed

CITATIONS

18

READS

11

3 AUTHORS, INCLUDING:



J. F. Douglas

National Institute of Standards and Technolo...

428 PUBLICATIONS 14,795 CITATIONS

SEE PROFILE



Karl F. Freed

University of Chicago

657 PUBLICATIONS 16,394 CITATIONS

SEE PROFILE

Lattice model of equilibrium polymerization. VI. Measures of fluid “complexity” and search for generalized corresponding states

Jack F. Douglas

Polymers Division, NIST, Gaithersburg, Maryland 20899, USA

Jacek Dudowicz and Karl F. Freed^{a)}

The James Franck Institute, University of Chicago, Chicago, Illinois 60637, USA

(Received 24 May 2007; accepted 24 August 2007; published online 11 December 2007)

Particle association in “complex” fluids containing charged, polar, or polymeric molecular species often leads to deviations from the corresponding state description of “simple” fluids in which the molecules are assumed to have relatively symmetric interactions and shapes. This fundamental problem is addressed by developing a minimal thermodynamic model of activated equilibrium polymerization solutions that incorporates effects associated with the *competition* between van der Waals and associative interactions, as well as features related to molecular anisotropy and many-body interactions. As a dual purpose, we focus on thermodynamic signatures that can be used to identify the nature of dynamic clustering transitions and the interaction parameters associated with these *rounded* thermodynamic transitions. The analysis begins by examining “singular” features in the concentration dependence of the osmotic pressure Π that generically characterize the onset of particle association. Because molecular self-assembly can strongly *couple* with fluid phase separation, evidence is also sought for associative interactions in the behavior of the second A_2 and third A_3 osmotic virial coefficients. In particular, the temperatures $T_{\Theta 2}$ and $T_{\Theta 3}$ where A_2 and A_3 , respectively, vanish are found to contain valuable information about the relative strength of the associative and van der Waals interactions. The critical temperature T_c for phase separation, the critical composition ϕ_c , and the rectilinear diameter A_d , describing the asymmetry of the coexistence curve for phase separation, along with the average cluster mass L_c and extent of polymerization Φ_c at the critical point, further specify the relevant interaction parameters of our model. Collectively, these characteristic properties provide a thermodynamic *metric* for defining fluid complexity and in developing a theoretically based corresponding state relation for complex fluids. © 2007 American Institute of Physics. [DOI: 10.1063/1.2785187]

I. INTRODUCTION

Associating fluids and their solutions exhibit a number of thermodynamic properties that distinguish them from “simple” fluids.¹ Fluids whose interactions are well described by a Lennard-Jones (LJ) interaction potential (e.g., argon, methane, etc.) are typical examples of “simple” fluids.² On the other hand, interparticle interactions in associating fluids are often highly *directional* (as in dipolar or multipolar fluids³) or exhibit “patchy” attractive regions on the particle surfaces (as in functionalized nanoparticles or proteins).^{4–7} Dynamic particle association is also prevalent for molecules and particles with disparate length scales for the repulsive and attractive forces.^{8,9} Anisotropy in molecular shape,¹⁰ in conjunction with shape fluctuations, can also induce a propensity toward dynamic particle association, but this phenomenon remains rather poorly understood. Recent static and dynamic light scattering measurements¹¹ have established the pervasive occurrence of supramolecular clustering at equilibrium, not only in polymeric fluids (such as ionomers, polyelectrolytes, and colloidal particle dispersions) but also in a variety of solutions of lower molecular mass elec-

trolytes, alcohol-water mixtures, and even in common organic solvent mixtures. Evidently, complex fluids are more of a rule than an exception.

In a previous paper,¹² we investigated fluids undergoing equilibrium polymerization as a generic minimal model of complex fluids, with particular focus on how particle association modifies the critical properties of these complex fluids. This prior study reveals that critical scattering properties, such as the correlation length ξ for collective composition fluctuations, the scattering intensity $S(0)$, and the width of the critical regime (defined by the Ginzburg number Gi), can all be strongly affected by particle clustering at equilibrium. The present work seeks to utilize this kind of information along with that for other thermodynamic properties (that are characteristic of associating fluids) to better classify and quantify complex fluids.

In order to place our goals in perspective and to define essential concepts, the remainder of this section reviews the establishment of the corresponding state description for simple fluids, the successes and failures in extending this model to complex fluids, the arguments supporting the need for including many-body interactions, and the definition of

^{a)}Electronic mail: k-freed@uchicago.edu

parameters that serve as measures of fluid “complexity” in a generalized corresponding state theory that is developed in subsequent sections.

A. In search of a corresponding state relation for complex fluids

The “principle of corresponding states” has long served as a framework for classifying fluid complexity and for predicting the properties of fluids, using only limited measured data (for a given fluid) and careful experimental studies of *reference fluids* over a wide range of thermodynamic conditions.^{13,14} This fundamental relation was originally derived by van der Waals,¹⁵ who noticed that the van der Waals equation of state could be expressed in terms of the critical parameters of the fluid (e.g., the critical temperature T_c and critical concentration φ_c), so that the equation of state exhibits no explicit dependence on the underlying molecular parameters describing the interactions. Moreover, these arguments formally imply that the thermodynamic and transport properties¹⁶ of all fluids should be determined from the same universal scaling functions. Thus, measurements of the properties for a *single fluid* suffice to establish these scaling functions for all representatives of this class of systems. Hence, any fluid can be compared to its “corresponding state” fluid at common values of reduced temperature and concentration (or reduced density for one-component systems). This simple, but amazingly general, idea has been one of the most fruitful concepts ever developed in liquid state theory in relation to practical engineering applications, far overtaking the impact of the van der Waals equation of state (whose rather inadequate description of real fluids was appreciated even in van der Waals time).¹³ Not until the midtwentieth century, after the proof of the existence of molecules, the development of quantum mechanics, and the elucidation of some essential aspects of molecular interactions, was the principle of corresponding states “derived” from statistical mechanics by using dimensional analysis or “scaling” ideas.^{13,17–19} This formal derivation only requires some reasonable assumptions that at least apply to certain simple fluids, such as those composed of molecules interacting with a *fixed* centrosymmetric intermolecular potential, as exemplified by the LJ potential. This analysis implicitly also assumes that the particles interact with a pairwise additive interaction potential that satisfies reasonable integrability properties to ensure the existence of thermodynamic properties (thereby excluding certain long range interactions¹³). Quantum effects are neglected in this formal treatment but can be readily incorporated.^{13,17,20} The derivation of the corresponding state relation for simple classical fluids represents the first application of “scaling theory” to fluid thermodynamics, and the scaling approach later proved fundamental for understanding the properties of fluids near their critical points and in diverse other “critical phenomena” contexts.^{21,22}

Although the predictive success of the corresponding state principle for fluid properties is impressive,¹³ it was soon realized that certain “associating” fluids, characterized by polar or other complex interactions that promote association,

could display appreciable deviations from the original two-parameter ($T/T_c, \varphi/\varphi_c$) corresponding state description.^{13,15} Later theoretical scaling arguments by Pitzer¹ indicate that *complex molecular shape* is a relevant factor for understanding deviations from the law of corresponding states in simple fluids because molecular shape influences the form of the intermolecular potential function ψ on which the theory of corresponding states is predicated. Polar and multipolar interactions are also recognized as obvious additional sources of deviations from the equation of state description of simple fluids, so that the general physical reasons for the breakdown of the corresponding state description of certain liquids are clear.¹ Accordingly, Pitzer¹ sought evidence for the influence of these factors on readily measured properties in order to develop a *metrology*¹³ for establishing a “generalized corresponding state principle.” In this attempt, Pitzer focused on the temperature dependence of the second virial coefficient A_2 , presumably because A_2 is one of the few thermodynamic properties that was exactly calculable for a wide range of potentials at the time and because A_2 is readily accessible experimentally.²³

Known properties of associating fluids provide additional clues of appropriate thermodynamic measures of association. For instance, the vapor phase density and the thermal conductivity of associating fluids have been noted to be “anomalously” high,¹³ effects attributed to the formation at low temperatures of dynamic molecular clusters (“double molecules”)^{24,25} since the time of van der Waals.^{13,15} The ramifications of particle association should then be especially apparent in the virial coefficients and related properties at low temperatures.¹ To extract this information effectively, Pitzer selected the fluid vapor pressure p , divided by its critical point value p_c , as the most convenient and accurately measurable property for establishing his new *metric* for developing a *generalized corresponding state* relation. In particular, a reduced reference temperature $T/T_c=0.7$ (below the critical temperature for phase separation) is chosen as a reference state since $p(T/T_c=0.7)/p_c$ happens to be close to unity in simple fluids¹ and because this is also a temperature range where A_2 and other fluid properties are sensitive to molecular association. The Pitzer “acentric factor,”¹

$$\omega \equiv p(T/T_c=0.7)/p_c - 1, \quad (1.1)$$

was then introduced as a measure of deviations from the simple or “perfect” fluid corresponding state description.¹ The term “acentric” simply refers to the interparticle potential ψ not being centrally symmetric, i.e., $\psi \neq \psi(|r|)$.

As in the original work of van der Waals, the concept of corresponding states implies that all long wavelength fluid properties Y of all fluids can be described through a generalized three-parameter scaling relation, $Y(T/T_c, \varphi/\varphi_c, x)$ or $Y(T/T_c, p/p_c, x)$, where x is a dimensionless variable characterizing the whole *equivalence class* of complex fluids.^{1,26} The initial work by Pitzer identifies Y with the “compressibility factor” Z (the pressure p normalized by p_0 its infinite dilution value, $Z \equiv p/p_0$), assuming that Z at a fixed reduced pressure can formally be decomposed into the sum of two independent terms,

$$Z(T/T_c; p/p_c) \approx Z^{(0)}(T/T_c; p/p_c) + \omega Z^{(1)}(T/T_c; p/p_c), \quad (1.2)$$

where $Z^{(0)}(T/T_c; p/p_c)$ is the simple fluid scaling function and $Z^{(1)}(T/T_c; p/p_c)$ is an additional “universal” contribution that accounts for the “acentric” character of the interparticle interactions. In practice, both $Z^{(0)}(T/T_c; p/p_c)$ and $Z^{(1)}(T/T_c; p/p_c)$ are determined and tabulated at a fixed p/p_c as polynomials in T_c/T . The formally truncated Taylor series expansion of $Z(T/T_c; p/p_c)$ in Eq. (1.2) implies that the deviations from the simple fluid equation of state are assumed to be sufficiently “small.” In addition to the analysis based on Z , an extensive treatment of the second and third virial coefficients has followed the same formal reasoning.^{27–31} The extension of Eq. (1.2) to condensed fluid mixtures involves replacing the gas pressure by the osmotic pressure Π and Z by the “osmotic compressibility factor” Z_Π . Equation (1.2) can be extended to properties other than Z , so that the one-component gas and condensed fluid mixtures share a common mathematical description. In the discussion below, we freely pass from a description of gas properties to those of fluid mixtures, based on this formal correspondence.

Although the specification of ω may appear somewhat contrived, this parameter has been measured and tabulated for a multitude of industrially important fluids and is a basic correlative parameter in the chemical processing industry.^{13,14} A further refinement of this generalized corresponding state idea lies in decomposing ω formally into *two separate components*, ϖ (the “true acentric factor”), which is related to molecular shape, and an “association factor” τ that is related to directional (in particular, dipolar) intermolecular interactions. Overall, this approach corresponds to the use of a *five parameter* corresponding state description of fluids since this generalized theory also includes a cross-term proportional to ϖ and τ .^{26,32,33} Despite the fact that these exercises in engineering scaling have clearly entered a Baroque era, they provide further evidence for the predictive power of the corresponding state concept and suggest that the proper treatment of interactions is the crucial ingredient in developing a more fundamental corresponding state description of complex fluids.

We address the problem of classifying complex fluids by formulating an analytical theory of an associating fluid having both directional (i.e., associative) and isotropic van der Waals interactions and by calculating the equation of state properties, albeit based on a mean field approximation as in the treatment of van der Waals for simple fluids. The modeling of fluids with associative interactions³⁴ and with competing van der Waals and associative interactions³⁵ initiated shortly after the work of van der Waals, so this field also has a long history.³⁶ Starting from a lattice model of fluid mixtures, Scott³⁷ and Wheeler *et al.*³⁸ have made many contributions to understanding the patterns of phase separation that occur in associating fluid mixtures. Recently, the theory of associating fluids has been in a rapid state of development,^{39–43} as new measurement and computational methods provide increased evidence for the formation of supermolecular structures that are distinct from those arising due to phase separation.

The present work confines attention to one-component fluids and incompressible fluid mixtures to avoid the presence of a multiplicity of (van der Waals) interaction parameters that characterize liquid-vapor transitions and the phase boundaries in binary mixtures.⁴⁴ Moreover, we find it convenient to use a lattice model, which simplifies the calculations considerably. The influence of many-body interactions on fluid miscibility is addressed in view of the work of Goldstein and co-workers,^{45,46} who provide convincing theoretical arguments and summarize experimental evidence that many-body interactions can be a source of deviations from corresponding state scaling.

Although our ultimate goal is to develop a generalized theory of corresponding states based on the direct analytic treatment of our model, the first task addressed here is to develop thermodynamic metrics for quantifying fluid complexity as the natural point of departure for theoretically attacking the generalized corresponding state problem.

B. Interparticle potential shape versus many-body interactions

The current investigation provides the opportunity to illuminate a well-known controversy over whether observed deviations from the corresponding state scaling description of simple fluids arise because of the “form” of the two-body potential (as argued by Pitzer¹) or rather from the existence of many-body interactions (as Goldstein and co-workers have claimed^{45,46}). We find that both groups are partially correct since A_2 also contains information about “many-body” interactions when the intermolecular interactions themselves are “complex”,⁴⁷ a possibility later suggested by de Bruyn and Goldstein.⁴⁶ Recall that Pitzer’s original arguments¹⁸ for the existence of corresponding states are predicated on the assumption that the particles interact with pairwise separable (two-body) potentials¹³ (see discussion below). Therefore, we incorporate a “three-body interaction” following a procedure similar to that used by Goldstein and co-workers^{45,46} for polarizable fluids and by Orofino and Flory⁴⁸ for polymer solutions where the three-body interactions derive from chain connectivity. While Goldstein and co-workers recognize the molecular polarizability as a source of three-body interactions, they neglect the influence of the polarizability on the second virial coefficient. In reality, molecular polarizability also influences A_2 , although this effect has not been subjected to much systematic investigation, presumably due to the associated computational difficulties.

Apart from polarizability effects,^{45,46} three-body effects in fluid mixtures also arise from the size and shape dissimilarity of the molecular species, a feature making these effects highly nonuniversal because their magnitude strongly depends on the solvent in which the polymer melt is dissolved. The influence of this kind of three-body interactions on fluid thermodynamics has been studied for polymer blends^{49,50} and for some other model mixtures of dissimilar sized molecules.⁵¹ Since there are evidently various contributors to the three-body interactions, we approach this complex matter pragmatically by subsuming them collectively into a single

extra adjustable three-body interaction parameter to hide these sins of omission.

It has recently become appreciated that three-body interactions can produce highly nontrivial variations (with temperature and polymer molar mass) of A_3 for polymer solutions, variations that are completely missed by the classical two-parameter theory of polymer excluded volume interactions.^{52,53} In particular, A_3 of flexible polymer solutions is generally found to be nonzero and *slowly varying* with T near $T_{\Theta 2}$ where A_2 vanishes. More specifically, A_3 actually *increases* somewhat below $T_{\Theta 2}$ and does not vanish at $T_{\Theta 2}$ as the two-parameter theory of polymer excluded volume predicts.^{54,55} Of course, a nonmonotonic temperature variation of A_3 is not specific to polymer fluids but is also observed for small molecule liquids where molecular anisotropy and directional interactions modulate the strength of the effect.⁵⁶ A full understanding of the observed variation in A_3 in polymer solutions is complicated by fluctuation effects, and an explanation of this phenomenon is one of the greatest challenges for the theory of polymer solutions.⁵⁷ Because many aspects of three-body interactions clearly require further study, modeling of this phenomenon in the present paper is necessarily idealized.

There is a long history relating to the extension of corresponding state ideas to polymeric liquids. Progogine *et al.*⁵⁸ have initiated this effort by using a lattice fluid model. Subsequent extensions of the theory involve off-lattice treatments.⁵⁹ An influential “cell model” of polymeric liquids by Nanda and Simha⁶⁰ has appeared at about the same time. These early models^{58–60} of polymeric fluids have later become superseded by polymeric equation of state models developed by Sanchez and Lacombe⁶¹ and then by Dickman and Hall,⁶² who creatively combine the lattice polymer and hard-sphere (off-lattice) models to obtain an explicit predictive equation of state for polymeric fluids. The most recent approaches to this problem include the lattice cluster⁶³ and integral equation⁶⁴ theories of polymer fluid thermodynamics that allow for a more realistic treatment of polymer chain structure. Another class⁶⁵ of advanced approaches to the equation of state properties of polymer melts is based on Wertheim’s perturbation theory.³⁹

The application of corresponding state or “scaling argument” reasoning has also been applied extensively to polymer solutions. After the initiation by Daoud and Jannik⁶⁶ and de Gennes,²² this field has been refined by Sanchez,⁶⁷ Chu and Wang,⁶⁸ and Muthukumar.⁶⁹ Recently, Anisimov *et al.*^{70,71} have incorporated three-body interactions into their equation of state description of polymer solutions, along with fluctuation contributions that extend beyond the mean field theory. These advances have led to a remarkably universal description of the phase boundaries of polymer solutions, reminiscent of the universal reduced variable description of simple fluids¹³ first deduced experimentally based on the van der Waals formal corresponding state idea. The above results provide great encouragement for the development of an equation of state theory of complex (associating) fluids.

C. Measures of fluid complexity

Although the ratios of the characteristic temperatures ($T_c, T_{\Theta 2}, T_{\Theta 3}$) are universal in simple fluids, they are obvious candidates for quantifying deviations from a corresponding state description of simple fluids, as well as potentially useful parameters for establishing a generalized equation of state. The four parameters ($\varphi_c, T_c, T_{\Theta 2}, T_{\Theta 3}$) should provide a better specification of the thermodynamics of these fluids than the usual two-parameter (T_c, φ_c) description of simple fluids, but it is unclear whether this set of parameters suffices for a complete description. The polymerization temperature T_Φ (see definition in the next section) is another obvious potential candidate for addition to this list since T_Φ characterizes the energy scale for association in a fashion similar to how T_c characterizes the energy scale for phase separation. Consequently, relating the molecular parameters of the model to the measurable characteristic parameters ($\varphi_c, T_c, T_{\Theta 2}, T_{\Theta 3}, T_\Phi$) represents an attractive strategy for developing a generalized corresponding relation.

Section II defines our activated equilibrium polymerization model for an associating fluid, along with essential properties required for establishing the equation of state and critical properties for this class of fluids. Section III describes our calculations of the transition lines that govern the self-assembly and that consequently are crucial for characterizing the fluid. Section 3 also summarizes our illustrative calculations for a series of metrics (briefly indicated above) of fluid complexity. With these tools in hand, the Helmholtz free energy and equation of state (for the reduced pressure) are expressed (see Sec. IV) in terms of observable quantities for a model fluid undergoing equilibrium polymerization. A generalized equation of state is then deduced from the closed analytic expressions (provided by our theory) following the van der Waals approach for developing the original two-parameter principle of corresponding states. As expected, the description of complex associating fluids requires introducing extra reduced variables.

II. ACTIVATED EQUILIBRIUM POLYMERIZATION MODEL FLUID WITH ASSOCIATIVE AND VAN DER WAALS INTERACTIONS

We focus on equilibrium polymerization since it is a simple and widely occurring example of a self-assembly transition involving an interplay between associative and van der Waals interactions, a basic feature of many complex fluids.¹² Our equilibrium polymerization theory^{12,72} is based on the standard Flory-Huggins model of polydisperse polymer solutions (at constant volume V) and on the assumption that the size distribution of chemically different polymer species is governed by thermodynamic equilibrium. The theory has been developed for three general models of association that differ in the constraints imposed on the polymerization process. While all three models have been analyzed in detail in a series of our papers,^{12,72–75} we confine attention here to a brief characterization and extension of the activated polymerization model in which the formation of thermally acti-

vated monomers is a necessary step for the initiation of polymerization. The simplest version of this model is described by the reaction scheme,⁷²



where the activated species M_1^* reacts only with nonactivated monomers M_1 to form dimers, but M_1^* does not participate in the successive chain propagation stages. The two corresponding equilibrium constants are defined as

$$K_a = \exp[-(\Delta h_a - T\Delta s_a)/(kT)] \quad (2.4a)$$

and

$$K_p = \exp[-(\Delta h_p - T\Delta s_p)/(kT)], \quad (2.4b)$$

for the activation and propagation processes, respectively. In order to minimize the number of adjustable parameters, a common equilibrium constant is prescribed for both reactions in Eqs. (2.2) and (2.3), based on the simplifying assumption that the enthalpies Δh_p and entropies Δs_p associated with dimer formation [Eq. (2.2)] and with the propagation process [Eq. (2.3)] are the same. The specification of the activated polymerization model then requires knowledge of only four free energy parameters, Δh_p , Δs_p , Δh_a , and Δs_a . The latter pair (i.e., the enthalpy Δh_a and entropy Δs_a of activation) controls the *sharpness* of the polymerization transition,⁷² while the former pair regulates the location of the transition,⁷² i.e., the magnitude of the polymerization transition temperature for a given initial monomer concentration φ_1^o .

The polymerization temperature is defined as the temperature T_Φ where the *extent of polymerization* $\Phi(T)$ (the fraction of monomers converted into polymers) exhibits an inflection point. For the activated polymerization model, T_Φ coincides with the temperature at which the specific heat achieves a maximum.⁷² The dependence of T_Φ on the initial monomer concentration φ_1^o is termed the “polymerization line,” which represents the boundary between monomer rich and polymer rich systems. (There are no coexisting phases in this type of thermodynamic transition as there are for phase separation.) Basic thermodynamic properties, such as the average polymer length, the extent of polymerization Φ , and the specific heat C_v , are functions of the initial monomer concentration φ_1^o , the temperature, and the energies ($\Delta h_p, \Delta h_a$) and entropies ($\Delta s_p, \Delta s_a$) of polymerization and activation. Below, we quote expressions for some basic solution properties that are discussed in Sec. III.

The average degree of polymerization (chain length) L or mass of the clusters for activated polymerization model equals

$$L = \frac{\varphi_1^o}{\varphi_1^o - CA^2/(1-A)^2}, \quad (2.5)$$

and the extent of polymerization or “order parameter” also has a closed form expression

$$\Phi = \frac{1}{\varphi_1^o} \frac{CA^2(2-A)}{(1-A)^2}. \quad (2.6)$$

The auxiliary variables appearing in these expressions are defined as

$$A = \varphi_1 K_p, \quad (2.7)$$

and

$$C = zK_a/(2\alpha K_p), \quad (2.8)$$

where φ_1 denotes the monomer concentration at equilibrium, z is the lattice coordination number, and the stiffness parameter α ranges from unity for stiff chains to $(z-1)$ for fully flexible chains.

In contrast to L and Φ , other thermodynamic properties of equilibrium polymer solutions, such as the Helmholtz free energy F , the osmotic pressure Π , isothermal osmotic compressibility κ , spinodal curves $T_s = T_s(\varphi_1^o)$, the second virial coefficient, and the theta temperature T_Θ , depend *explicitly* on the van der Waals (Flory-Huggins parameter in a lattice model context) effective interaction parameter $\chi_o = \varepsilon_{FH}/T$, as well as on the energetic parameters governing dynamic particle clustering, Δh_p , Δh_a , Δs_p , and Δs_a .⁷² The dependence on these parameters is made apparent in the following expressions:⁷²

$$\frac{F}{N_1 kT} \equiv \frac{f}{kT} = (1 - \varphi_1^o) \ln(1 - \varphi_1^o) + \varphi_1^o \ln \varphi_1 + (1 - \varphi_1^o) \varphi_1^o \chi_o + \frac{CA^2}{(1-A)^2}, \quad (2.9)$$

$$\frac{\Pi v_{\text{cell}}}{kT} = -\ln(1 - \varphi_1^o) - (\varphi_1^o)^2 \chi_o - \frac{CA^2}{(1-A)^2}, \quad (2.10)$$

$$\kappa = \frac{v_{\text{cell}}}{kT} \frac{1}{\varphi_1^o} \left[\frac{1}{1 - \varphi_1^o} - 2\varphi_1^o \chi_o - \frac{2CAK_p}{(1-A)^3(1+K_a) + CK_p(A^3 - 3A^2 + 4A)} \right]^{-1}, \quad (2.11)$$

$$A_2 = \frac{1}{2} - \chi_o - \frac{CK_p^2}{(1+K_a)^2}, \quad T_\Theta \equiv T_{\Theta 2} = T(A_2 = 0), \quad (2.12)$$

$$\frac{1}{\varphi_1^o + \frac{2CA^2}{(1-A)^3}} + \frac{1}{1 - \varphi_1^o} - 2\chi_o = 0 \quad (\text{spinodal curve}), \quad (2.13)$$

where v_{cell} is the average volume of a monomer and solvent molecule (taken to be independent of temperature), N_l is the total number of monomers and solvent molecules ($V = N_l v_{\text{cell}}$), $\varepsilon_{FH} = \varepsilon_{mm} + \varepsilon_{ss} - 2\varepsilon_{ms}$ is the “strength” of the van der Waals interactions, and where the subscripts *mm*, *ss*, and *ms* on the van der Waals energies $\{\varepsilon_{\alpha\beta}\}$ label the monomer-monomer, solvent-solvent, and monomer-solvent pairs, respectively. The assumption of a single binary van der Waals interaction parameter ε_{FH} is appropriate for incompressible binary mixtures, so that our model applies to liquid-liquid

phase separation processes under conditions far from any liquid-vapor phase boundary. The prediction that A_2 is a function of the equilibrium constant for association also emerges from other models of associating fluids (e.g., see Ref. 76).

The third osmotic virial coefficient of our model associating fluid equals

$$A_3 = \frac{1}{3} + \frac{2CK_p^3}{(1+K_a)^3} \left[\frac{2CK_p}{1+K_a} - 1 \right], \quad (2.14)$$

and $T_{\Theta 3}$ is defined as the temperature at which A_3 vanishes, i.e., $T_{\Theta 3} = T(A_3 = 0)$. Equation (2.14) implies that in the absence of association, A_3 is simply positive and invariant to temperature. However, the lack of a perfect equivalence between the shapes of the molecular species breaks the inversion symmetry responsible for this effect. Mathematically, shape anisotropy leads to three-body interactions that make A_3 temperature dependent, even in the absence of molecular association (see Appendix A).

The coexistence curve (binodal) for a constant volume V , incompressible solution of an associating species is determined from the equality, respectively, of the exchange chemical potentials $\mu_{\text{exch}}^{(I)}$ and $\mu_{\text{exch}}^{(II)}$ and of the osmotic pressures $\Pi^{(I)}$ and $\Pi^{(II)}$ in the two coexisting phases I and II. The exchange chemical potential is the difference between the chemical potential μ_1^o of a monomer of the associating species (before polymerization) and the chemical potential μ_s of a solvent molecule,

$$\mu_{\text{exch}} = \mu_1^o - \mu_s = \left. \frac{\partial F}{\partial n_1^o} \right|_{T,V} = \left. \frac{\partial f}{\partial \varphi_1^o} \right|_{T,N_1}, \quad \varphi_1^o = \frac{n_1^o}{N_1}, \quad (2.15)$$

and can be readily evaluated from the free energy expression in Eq. (2.9), thereby giving

$$\mu_{\text{exch}}^{(\alpha)} = \ln(\varphi_1^o)^{(\alpha)} + \ln[1 - (\varphi_1^o)^{(\alpha)}] + [1 - 2(\varphi_1^o)^{(\alpha)}]\chi_o, \quad (2.16)$$

$$\alpha \equiv \text{I, II.}$$

The osmotic pressure $\Pi^{(\alpha)}$ in the coexisting phase α simply follows from Eq. (2.10) by formally replacing φ_1^o by $(\varphi_1^o)^{(\alpha)}$.

The *rectilinear diameter* provides a basic measure of the shape of the coexistence curve and is determined by simply averaging the compositions φ^+ and φ^- of the two coexisting phases (where the superscripts $+$ and $-$ refer to the concentrated and dilute phases, respectively). Over a temperature range of about 30 K below the critical point ($T_c - T \leq 30$ K), the average composition is normally found to vary linearly with temperature to a good approximation,^{19,77-80}

$$(\varphi^+ + \varphi^-)/(2\varphi_c) = 1 + A_d(1 - T/T_c), \quad (2.17)$$

where A_d is the rectilinear diameter slope. For simple fluids, A_d is a constant, which approximately equals $\frac{3}{4}$ for one-component fluids.¹⁹ A number of theories^{19,70,80,81} predict deviations from this linear behavior in a relatively narrow temperature range near the critical point where critical fluctuations affect the phase separation process appreciably.^{81,82}

We have explicitly derived the molecular origins of such three-body contributions to the free energy of mixing in our previous investigations of the thermodynamic properties of polymer blends with structured monomers.^{49,50} In addition to three-body interactions arising from the dissimilarity of monomer shape and flexibility, three-body effects can also stem from molecular polarizability^{45,46} and other collective interactions.

The incorporation of three-body terms into our free energy must be performed in an internally consistent theoretical manner, a matter which has been considered previously within the lattice cluster theory and its simplified versions.^{49,50} We begin by noting that the interaction portion $f_{\chi}/(kT)$ of the system's Helmholtz free energy $f/(kT)$ [see Eq. (2.9)] is represented by the product $\varphi_1^o(1 - \varphi_1^o)\chi_o$. The introduction of a three-body or "ternary" interaction (see Appendix A) implies that $f_{\chi}/(kT)$ is a sum of three contributions,

$$f_{\chi}/(kT) = \varphi_1^o(1 - \varphi_1^o)[\chi_o + \chi_{mms}\varphi_1^o + \chi_{mss}(1 - \varphi_1^o)], \quad (2.18)$$

where χ_{mms} and χ_{mss} designate the three-body interaction parameters within monomer-monomer-solvent and monomer-solvent-solvent triads, respectively. Rearranging Eq. (2.18) then yields

$$f_{\chi}/(kT) = \varphi_1^o(1 - \varphi_1^o)[\chi + \chi_{\text{extra}}\varphi_1^o], \quad (2.19)$$

where $\chi \equiv \chi_o + \chi_{mss}$ and $\chi_{\text{extra}} \equiv \chi_{mms} - \chi_{mss}$. The presence of the extra term in Eq. (2.19) then leads to the following modification of Eqs. (2.10)–(2.16):

$$\begin{aligned} \frac{\Pi v_{\text{cell}}}{kT} = & -\ln(1 - \varphi_1^o) - (\varphi_1^o)^2[\chi - \chi_{\text{extra}}] \\ & - 2(\varphi_1^o)^3\chi_{\text{extra}} - \frac{CA^2}{(1-A)^2}, \end{aligned} \quad (2.20)$$

$$\begin{aligned} \kappa = \frac{v_{\text{cell}}}{kT} \frac{1}{\varphi_1^o} \left[\frac{1}{1 - \varphi_1^o} - 2\varphi_1^o[\chi - \chi_{\text{extra}}] - 6(\varphi_1^o)^2\chi_{\text{extra}} \right. \\ \left. - \frac{2CAK_p}{(1-A)^3(1+K_a) + CK_p(A^3 - 3A^2 + 4A)} \right]^{-1}, \end{aligned} \quad (2.21)$$

$$A_2 = \frac{1}{2} - (\chi - \chi_{\text{extra}}) - \frac{CK_p^2}{(1+K_a)^2}, \quad (2.22)$$

$$A_3 = \frac{1}{3} - 2\chi_{\text{extra}} + \frac{2CK_p^3}{(1+K_a)^3} \left[\frac{2CK_p}{1+K_a} - 1 \right], \quad (2.23)$$

$$\begin{aligned} \frac{1}{\varphi_1^o + \frac{2CA^2}{(1-A)^3}} + \frac{1}{1 - \varphi_1^o} - 2\chi \\ + 2\chi_{\text{extra}}(1 - 3\varphi_1^o) = 0 \quad (\text{spinodal curve}), \end{aligned} \quad (2.24)$$

$$\begin{aligned} \mu_{\text{exch}}^{(\alpha)} = \ln(\varphi_1^o)^{(\alpha)} + \ln[1 - (\varphi_1^o)^{(\alpha)}] + [1 - 2(\varphi_1^o)^{(\alpha)}]\chi \\ + 2(\varphi_1^o)^{(\alpha)}\chi_{\text{extra}} - 3[(\varphi_1^o)^{(\alpha)}]^2\chi_{\text{extra}}. \end{aligned} \quad (2.25)$$

The inclusion of three-body interactions into the system's Helmholtz free energy not only modifies A_3 , so that it

now depends on the van der Waals interaction energy ε_{FH} , but it also modifies A_2 . The osmotic pressure Π , isothermal osmotic compressibility κ , and the critical temperature and critical composition ϕ_c for phase separation are all altered by the presence of three-body interaction effects, and evidently a physical criterion is needed to determine the magnitude of the three-body interactions in the theory. Note that Eqs. (2.22) and (2.23) apply to equilibrium polymer solutions in which the solvent is the majority species. Generalization to the case where the solvent becomes the minority species is straightforward (see Appendix A).

III. ILLUSTRATIVE CALCULATIONS FOR A MODEL COMPLEX ASSOCIATING FLUID

A. Activated equilibrium polymerization model

Our calculations are performed for an equilibrium polymerization model in which the first step of polymerization involves thermal activation, so that the sharpness (degree of transition “rounding”⁷⁵) of the polymerization transition may be controlled by varying the equilibrium constant for the activation process. This variability in transition sharpness is important for a general discussion since micelle formation and gelation are normally rather sharp self-assembly thermodynamic transitions, while other transitions, such as the assembly of colloidal magnetic particles, can be quite broad. Consequently, the equilibrium constant for thermal activation is chosen in illustrative calculations to ensure the appearance of a relatively sharp (“cooperative”) polymerization transition.

With these general remarks in mind, consider a polymerizing monomer-solvent system on a three dimensional ($d=3$) cubic lattice with a coordination number $z=6$ and restrict attention to systems in which both polymerization and activation processes proceed upon cooling, which in turn implies that all four free energy parameters are negative. Unless otherwise stated, the activated polymerization model is specified by the free energy parameters, $\Delta h_p = -35$ kJ/mol, $\Delta h_a = -35$ kJ/mol, $\Delta s_p = -105$ J/(mol K) and $\Delta s_a = -210$ J/(mol K), which lead to a reasonably sharp polymerization transition and to the saturation of the average polymer length at low temperatures.¹² Similar parameter sets ($\Delta h_p, \Delta s_p, \Delta h_a, \Delta s_a$) have been employed in a recent analysis of the scattering properties of equilibrium polymer solutions,¹² thereby facilitating comparisons to this former work. Clusters are treated, for simplicity, as rigid chains, i.e., the factor α in Eq. (2.8) is set to unity. Since only two of the adjustable parameters ($\chi_{\text{mms}}, \chi_{\text{mss}}$, and χ_o) in Eqs. (2.19) and (2.25) are independent, we assume that $\chi_{\text{mss}}=0$, which implies that $\chi = \varepsilon_{\text{FH}}/T$ and $\chi_{\text{extra}} = \gamma \varepsilon_{\text{FH}}/T$ (see Appendix A), and the van der Waals exchange energy ε_{FH} is taken as $\varepsilon_{\text{FH}} = 177$ K following the choice in Ref. 75. The amplitude γ of the three-body interactions is fixed as $\gamma=0.17$ by the condition that the ratio $r_o = T_\theta^o/T_c^o$ of the theta temperature T_θ^o to the critical temperature equals 3 for the monomer-solvent mixture with no polymerization present. In the absence of three-body interactions ($\gamma=0$), the computed ratio $r_o = T_\theta^o/T_c^o$ achieves the lattice mean field value of 4. Experiments reveal, however, that one-component fluids that lack

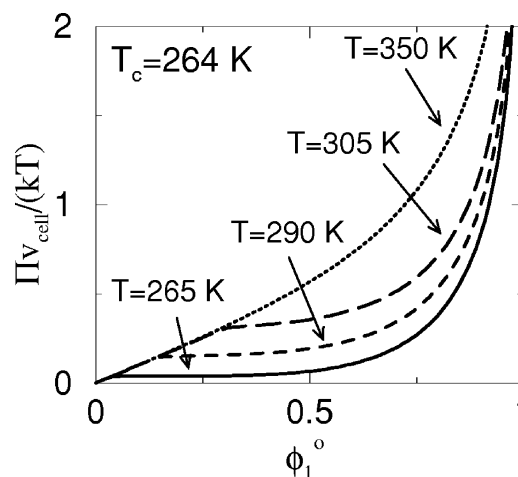


FIG. 1. Typical variation of the dimensionless osmotic pressure $\Pi v_{\text{cell}}/(kT)$ with the initial monomer composition ϕ_1^o for equilibrium polymer solutions at temperatures above the critical temperature. The curves in the figure are computed for the activated equilibrium polymerization model described in the text and specified by $\Delta h_p = \Delta h_a = -35$ kJ/mol, $\Delta s_p = (1/2)\Delta s_a = -105$ J/(mol K), $\varepsilon_{\text{FH}} = 177$ K, $\gamma = 0.17$, and $\alpha = 1$ (i.e., clusters are assumed to be rigid structures). Unless stated otherwise, the same free energy parameters Δh_p , Δh_a , Δs_p , and Δs_a , the exchange energy ε_{FH} , the factor α , and the factor γ (that quantifies the strength of three-body interactions) are used in computations summarized in Figs. 2–11.

perfect particle-hole exchange symmetry^{81,83} are characterized by a ratio $r_o \approx 2.64$, which is nearly universal for simple fluids.¹⁹ (The absence of particle-hole exchange symmetry in one-component fluids and molecular exchange symmetry in fluids mixtures leads to a number of subtle effects that can not be recovered by simply introducing an effective three-body interactions, so this method of fixing our three-body interaction parameter is clearly an approximation. Wang and Anisimov⁸¹ have recently systematically investigated the consequences of particle-hole asymmetry on the critical properties of fluids.) Of course, critical fluctuations affect T_c by an amount that can be as large as 25% of the mean field theory estimate in three dimensions,⁸² explaining our settling on a reasonable estimate of $r_o = 3$ in the illustrative calculations.

B. Singular equation of state features in associating fluids

The equation of state of a solution relates the osmotic pressure Π to the concentration (volume fraction ϕ) of the associating species and provides a natural vehicle for examining thermodynamic “signatures” of associating fluids. Generically, Π of these complex fluids increases with ϕ in a convex fashion at low concentrations in the one-phase region, but in contrast to simple fluids, Π then varies relatively slowly with ϕ following the onset of particle clustering. Figure 1 illustrates this characteristic behavior for a model associating fluid, a behavior which not only occurs for equilibrium polymerization but also is evident in micelle formation,⁸⁴ gel-forming associating polymers,⁸⁵ gelation in exfoliated clay solutions⁸⁶ and polyelectrolyte solutions,^{87,88} etc. The concentration at which this “transition” appears in

the dependence of Π has often been identified^{84–86} with the critical concentration for the type of self-assembly involved (micelle formation,⁸⁴ gelation,^{85,86} etc.).

De Gennes⁸⁹ has introduced an *ad hoc*, ‘*m*-cluster’ model to describe the phase separation of a particular associating fluid (polyethylene oxide in water). Within this model, the polymer’s second virial coefficient A_2 is assumed to be positive, while higher order virial coefficients are taken to be negative, thereby predicting an unusual type of phase separation when these higher virial coefficients become sufficiently negative. (This model contrasts with claims that A_3 of all real fluids must be positive at the theta or Boyle point at which A_2 vanishes.⁹⁰) De Gennes’ model leads to the peculiar notion of polymers actually being *swollen* in both coexisting phases of the phase separated solution, a situation that would have profound consequences if true.⁸⁹ At any rate, the combination of a positive A_2 with a negative A_3 yields a potentially attractive mathematical explanation for the turnover in the concentration dependence of Π (at higher concentrations) for associating fluids (see Fig. 1), although de Gennes’ model⁸⁹ obviously requires mathematical and physical justification.

Qualitative support for de Gennes’ radical arguments emerges from experiments⁸⁷ in which variable amounts of CaCl_2 salt are added to the Na salt solutions (10 mM) of various polyelectrolytes [DNA solutions,⁸⁸ sulfonated polystyrene solutions (SPS),⁸⁸ and polyacrylate solutions of relatively high charge density⁸⁷]. Adding salt is an established method of reducing the solvent quality of these solutions.⁹¹ Increasing the Ca salt concentration φ_{Ca} ultimately leads to phase separation. The value of A_2 , deduced from a fit of the Flory-Huggins theory to the osmotic pressure data, is found to be *positive* and nearly invariant, while A_3 diminishes with increasing φ_{Ca} and then becomes negative, signaling the onset of phase separation. These observations suggest that there might be some fundamental truth in de Gennes heuristic *m*-cluster model arguments. Thus, we examine this issue systematically within the framework of our analytical equilibrium polymer theory by testing the possibility that A_3 can vanish before A_2 in systems with sufficiently strong associative interactions and with both activation and polymerization processes proceeding upon cooling. Because the dynamic association of polymer chains in highly charged polyelectrolyte solutions is an established phenomenon,^{92–98} qualitative comparison to equilibrium polymerization theory is reasonable. Motivated by the observations and arguments just mentioned, the “theta temperatures” of the osmotic virial coefficients A_2 and A_3 ($T_{\theta 2}$ and $T_{\theta 3}$, respectively) are also computed for our activated equilibrium polymerization model (see Sec. III D).

C. Self-consistent determination of polymerization transition lines

An additional goal of the present work involves devising improved means for determining the energetic parameters and the transition lines governing thermodynamic self-assembly transitions. Clearly, the energetic parameters must somehow be related to the equation of state of these complex

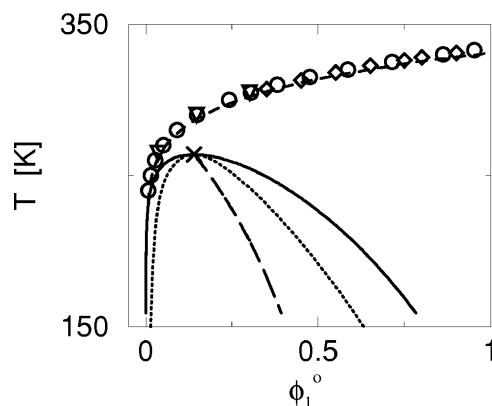


FIG. 2. The polymerization transition line $T_p = T_p(\varphi_1^o)$ (dashed line), coexistence curve (dotted line), and the spinodal curve (solid line) for a model fluid exhibiting activated equilibrium polymerization in the intermediate coupling regime (defined in the text) where the polymerization transition temperature at the critical composition and the critical temperature are comparable in magnitude. The critical point is indicated by a cross, while other symbols denote estimates of the polymerization line that are obtained from the composition variation of the average polymerization index $L(\varphi_1^o, T = \text{const})$ (circles), the isothermal osmotic compressibility $\kappa kT/v_{\text{cell}}(\varphi_1^o, T = \text{const})$ (diamonds), and the osmotic pressure $\Pi v_{\text{cell}}/kT(\varphi_1^o, T = \text{const})$ (triangles). The coexistence curve (dotted line) is evidently asymmetric, reflecting the “polymeric” nature of the fluid at the critical temperature, and the rectilinear diameter (long dashed line) displays a large slope. The curvature of the rectilinear curve derives from the three-body interactions that generally arise from size anisotropy (between a solvent molecule and a monomer of the associating species) or from the molecular polarizability (see text).

fluids. The “polymerization line” $T_p(\varphi_1^o)$ is one of the most frequently studied thermodynamic properties of associating liquids since it provides information on the magnitude of the enthalpy Δh_p and entropy Δs_p of assembly. Recent simulations of these transition lines for model associating fluids reveal how the molecular interaction parameters are related to the interaction potential.^{3,7,99}

Various methods of estimating the polymerization line $T_p = T_p(\varphi_1^o)$ have been suggested in our previous studies^{73,75} of “living” polymerization where dynamic chain growth is induced by the presence of a chemical “initiator” whose concentration plays a similar role to the equilibrium constant for a monomer activation in the activated polymerization model. These methods are again examined here to test their validity and accuracy for systems undergoing activated equilibrium polymerization.

The first method of locating T_p involves analyzing the average degree of polymerization $L(\varphi_1^o)$ for a fixed temperature T as a function of φ_1^o and extrapolating the curve for $L(\varphi_1^o)$ to zero (see Fig. 3 of Ref. 73) to locate $\varphi_{1,\text{cpc}}^o$, below which no polymer growth exists. The results of this procedure are designated by circles in Fig. 2 and are rather consistent with the estimates of T_p from the inflection point in $\Phi(T)$ and, equivalently, the maximum in $C_v(T)$, which are indicated by short dash lines in Fig. 2.

Next, consider the sharp maximum in the dimensionless isothermal osmotic compressibility $\kappa(kT/v_{\text{cell}})$ that occurs at a fixed temperature when this quantity is plotted against the initial monomer concentration φ_1^o (see Fig. 3 of Ref. 75 where this thermodynamic feature is discussed for living polymer solutions). The diamonds in Fig. 2 demonstrate that this criterion also provides an effective means of locating the

polymerization transition line. The last method of determining $T_p(\varphi_1^0)$ is derived from the location of the onset of the plateau in the dimensionless osmotic pressure $\Pi v_{\text{cell}}/(kT)$ in Fig. 1, where the plateau position is obtained by extrapolating the horizontal portion of the curve for $\Pi v_{\text{cell}}/kT(\varphi_1^0, T = \text{const})$ until it crosses the linear part. This estimate of $T_p(\varphi_1^0)$ is indicated in Fig. 2 by triangles. It is encouraging that all these methods of locating the polymerization line are self-consistent to a high approximation. The polymerization line is evidently as basic a quantity for characterizing associating fluids as the coexistence curve is for describing a fluid's phase separation. The spinodal (solid line in Fig. 2) and coexistence (dotted line in Fig. 2) curves are also included to emphasize the competition between polymerization and phase separation. The rectilinear diameter [see Eq. (2.17)] curve, reflecting the average of the coexistence curve branches, is indicated in Fig. 2 as a long dashed line. The high degree of polymerization that develops near the critical point is responsible for the striking asymmetry of the coexistence curve, a feature common to many complex fluids.¹² The rectilinear diameter in Fig. 2 is evidently only approximately linear over a limited temperature range [$(T_c - T) \leq 30$ K]. Our additional calculations (not shown here) indicate that this curvature is primarily controlled by the magnitude of the three-body interactions since the curvature essentially vanishes as the ternary interactions approach zero. Thus, the presence of many-body effects is reflected in the shape of the phase boundary. Consistent with this general observation, the rectilinear diameter curves of rubidium and other metallic fluids (that are expected to exhibit large three-body interactions associated with polarizability effects) are found^{45,46,80,100} to possess highly curved rectilinear diameters.

Inspecting the methods for determining the polymerization line in Fig. 2 suggests, however, that osmotic pressure measurements can be used only to estimate the transition line at relatively low initial monomer concentrations since II exhibits a “plateau” only over a limited temperature range above T_c . Evidently, the critical temperature T_c for phase separation in Fig. 2 lies below the polymerization temperature T_p for concentrations well above the critical concentration φ_c , a situation that is not generally true since the magnitudes of the association energy Δh_p and the entropy Δs_p , as well as other model parameters, influence the location of the polymerization transition line.^{12,72,74}

We have previously^{12,72} defined three main interaction regimes: (a) a “weak coupling” regime I in Fig. 3 where the magnitude of the sticking energy Δh_p is so small that T_c is practically identical to the critical temperature T_c^0 of a “bare” monomer-solvent system with no association present, (b) a “strong coupling” regime III in Fig. 3 where $|\Delta h_p|$ is so large that T_c saturates to a constant value, $T_c^\infty \equiv T_c(\Delta h_p \rightarrow \infty)$, and (c) an intermediate coupling regime II in Fig. 3 where T_c lies intermediate between T_c^0 and T_c^∞ . To clarify this concept within the context of the activated equilibrium polymerization model, T_c is displayed as a function of $|\Delta h_p|$ in Fig. 3 where the interaction regimes are indicated. The above criterion for specifying the three regimes departs from that based on the location of the polymerization line with respect to the

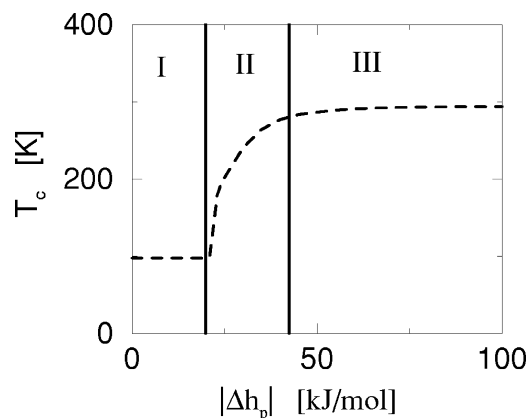


FIG. 3. The critical temperature for the phase separation of equilibrium polymerization solutions as a function of the polymerization energy Δh_p and computed for the activated polymerization model described in the text. The existence of three different regimes in the qualitative behavior of $T_c(\Delta h_p)$ provides a convenient criterion for defining the weak, strong, and intermediate coupling regimes of associative interactions, which are labeled in the figure by I, II, and III, respectively.

phase boundary^{12,74} and employed previously by us for the free association (FA) and I models of equilibrium polymerization. The activated polymerization model can exhibit two polymerization lines due to a strong competition between activation and polymerization, a phenomenon that does not occur in the other equilibrium polymerization models where the strong, weak, and intermediate coupling regimes simply correspond to the situation where the polymerization temperature T_p at the critical composition φ_c is above, below, or coincident with T_c , respectively.

D. Second and third virial theta temperatures, $T_{\theta 2}$ and $T_{\theta 3}$

The next essential reference temperature for polymer solutions is the theta temperature $T_{\theta 2}$ defined as the temperature at which A_2 vanishes. In analogy to $T_{\theta 2}$, we define the temperature $T_{\theta 3}$ at which the third virial coefficient vanishes. (The utility of $T_{\theta 3}$ for characterizing associating fluids has only recently been realized.⁵⁶) The importance of $T_{\theta 3}$ can be appreciated by analyzing the quite surprising temperature variation of A_2 and A_3 . (We did not think to consider $T_{\theta 3}$ until confronted with the polyelectrolyte data discussed in Sec. III A.) The temperature dependence of these virial coefficients for the weak, strong, and intermediate coupling regimes is indicated in Figs. 4(a)–4(c), respectively. Nothing unusual appears in the weak coupling regime, which basically corresponds to the case of simple liquids where A_2 vanishes upon cooling well before A_3 (i.e., $T_{\theta 2} \equiv T_\theta > T_{\theta 3}$). However, an opposite trend is found in the strong coupling regime where A_3 vanishes first upon decreasing the temperature. Both types of behavior are possible for the intermediate coupling regime, depending on $|\Delta h_p|$. Figure 4(c) presents a particular case where both A_2 and A_3 vanish at approximately the same temperature. Figures 4(d)–4(f) obtained by replotting Figs. 4(a)–4(c), respectively, show, in turn, the dependence of A_2 and A_3 on $1/T$, which is relevant to our discussion in the next section.

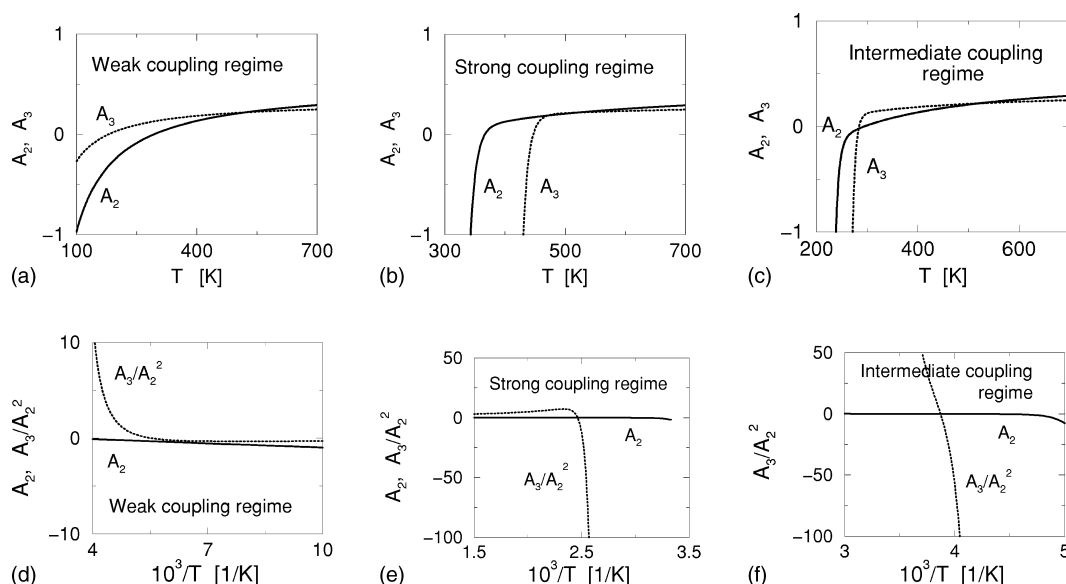


FIG. 4. (a) Temperature variation of the second (A_2) and third (A_3) virial coefficients for equilibrium polymer solutions in the weak coupling regime ($\Delta h_p = -10$ kJ/mol), as computed for the activated polymerization model described in the text. (b) Temperature variation of the second (A_2) and third (A_3) virial coefficients for equilibrium polymerization solutions in the strong coupling regime phase ($\Delta h_p = -70$ kJ/mol) as computed for the activated polymerization model described in the text. (c) Temperature variation of the second (A_2) and third (A_3) virial coefficients for equilibrium polymerization solutions in the intermediate coupling regime between polymerization and phase separation ($\Delta h_p = -37.5$ kJ/mol) as computed for the activated polymerization model specified in the text. The second and third virial coefficients as functions of the inverse temperature $1/T$ for (d) the weak, (e) the strong, and (f) the intermediate coupling regimes.

E. Strong coupling and evidence for the inversion of $T_{\Theta 2}$ and $T_{\Theta 3}$

The inversion of the order of $T_{\Theta 2}$ and $T_{\Theta 3}$ is certainly the kind of singular phenomenon that is useful for fingerprinting associating fluids, as illustrated by a closer examination of this phenomenon in comparison with the data for the polyelectrolyte system mentioned before. Experimental data for the osmotic virial coefficients for a highly charged polyacrylate polyelectrolyte gel are presented in Fig. 5(a). (The preparation and molecular characteristics of these gels are described by Horkay *et al.*,^{87,88,92} who analyze their osmotic pressure data in terms of Flory-Huggins interaction parameters [see Fig. 5(a)] rather than in terms of virial coefficients.) The data are illustrative of a general phenomenon, and the same qualitative trends have been observed in DNA gels and other highly charged polyelectrolytes.^{87,88,92} Since the measurements are performed for cross-linked gels, only the mixing component Π_{mix} of the total osmotic pressure Π is used in determining the virial coefficients for the various concentrations of CaCl_2 [expressed in mM units in Fig. 6 of Ref. 87(a)]. The effective A_2 and A_3 of Fig. 5(b) are determined from fits of the osmotic data and closely accord to those extracted from a polynomial expansion of Π_{mix} , but the former fits are restricted to a narrower temperature range and thus are more uncertain.

It is well recognized that adding divalent salts to polyelectrolyte solutions reduces the solvent quality^{91,101–103} and that if enough salt is added, phase separation occurs, much as neutral polymer solutions separate upon the decrease of the temperature. More specifically, Flory predicted that the interaction parameter χ for polyelectrolyte solutions with a moderate amount of added salt (corresponding to the experimental samples under discussion) has an additional contribution

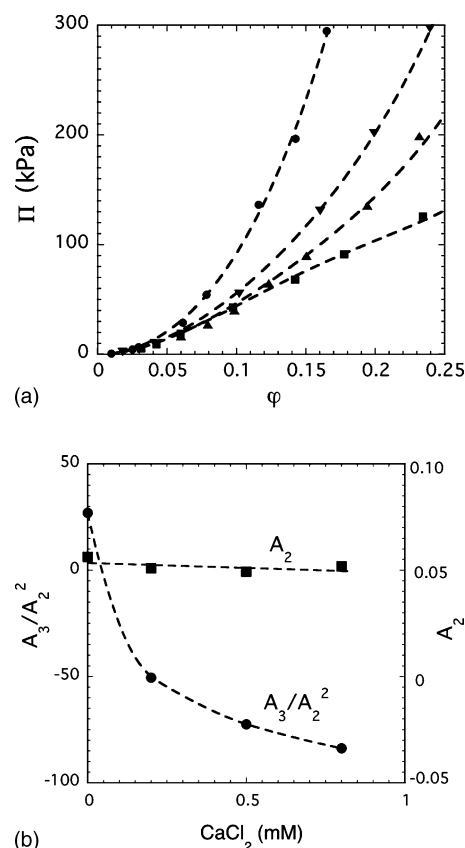


FIG. 5. (a) The mixing component Π_{mix} of the osmotic pressure Π as a function of polymer volume fraction ϕ for polyacrylate gels in equilibrium with solutions of NaCl and CaCl_2 . Different curves correspond to different salt concentrations, as in Fig. 6 of Ref. 87(a). (b) The second virial coefficient A_2 and the ratio A_3/A_2^2 (where A_3 is the third virial coefficient) as functions of the concentration of CaCl_2 . The virial coefficients are obtained from fits of the FH expression for the osmotic pressure to the experimental data shown in (a).

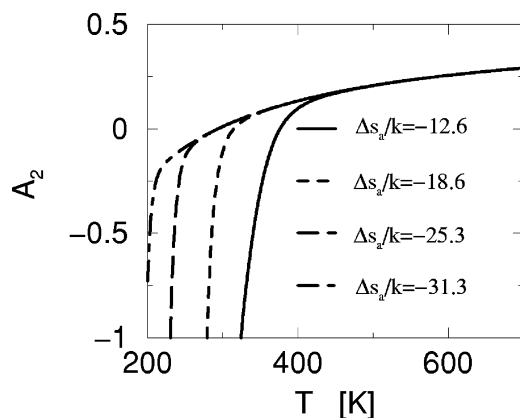


FIG. 6. Temperature variation of the second virial coefficient A_2 of equilibrium polymer solutions as computed for different values of the activation entropy Δs_a that are specified in the figure [$\Delta s_p = -105$ J/(mol K)].

from the ions that scales inversely to the ionic strength.^{101,104} (More recent works by Warren,¹⁰⁵ Raspaud *et al.*,¹⁰³ Olvera de la Cruz *et al.*,¹⁰⁶ and Muthukumar¹⁰⁷ arrive at the same scaling expression between the polyelectrolyte contribution to the effective polymer-polymer interaction parameter χ and the ionic strength.) Increasing the Ca salt concentration φ_{Ca} elevates the ionic strength and accordingly should reduce the solvent quality. Direct measurements strongly support Flory's estimate of the change of χ with salt concentration, both for monovalent and divalent salts, justifying this interpretation of the “salting out” effect.^{91,101–103} Thus, increasing φ_{Ca} can roughly be thought of as reducing the effective temperature T (or increasing χ or $1/T$). Consequently, the variation of A_2 and A_3/A_2^2 with salt concentration for polyacrylate hydrogels [see Fig. 5(b)] is appropriately compared to the changes in A_2 and A_3/A_2^2 for our equilibrium polymerization model [see Fig. 4(e)]. This comparison reveals that A_3 vanishes before A_2 both for the activated equilibrium polymerization model and the polyelectrolyte system upon a reduction of solvent quality. Because the original data for $\Pi_{\text{mix}}(\varphi, c_s = \text{const})$ are analyzed in terms of generalized χ parameters,⁸⁷ instead of A_2 and A_3 , this unusual trend for the virial coefficients was not recognized.

The relevance of the activated equilibrium polymerization model to studies of polyelectrolytes deserves comment. Activated processes are prevalent in charged and multipole interaction systems as the charged particles tend to form low energy “multiplet” clusters of particular symmetries (dipolar, quadrupolar, etc.),^{108–110} which in turn aggregate into larger scale self-assembled structures.³ This initial clustering into multiplet structures can be considered as an activated process that regulates the larger scale self-assembled structures,^{109,110} which in turn may exert a large influence on the phase behavior.¹¹¹ In short, the description of polyelectrolyte solutions is really more complicated than that emerging from the original Flory theory.^{101,104}

The conventional rule of thumb, according to which the second osmotic virial coefficient simply reflects the interaction of only two particles, does not generally apply to complex fluids where many-body effects can significantly contribute to A_2 . For instance, our equilibrium polymer model depends not only on the strength of the three-body interac-

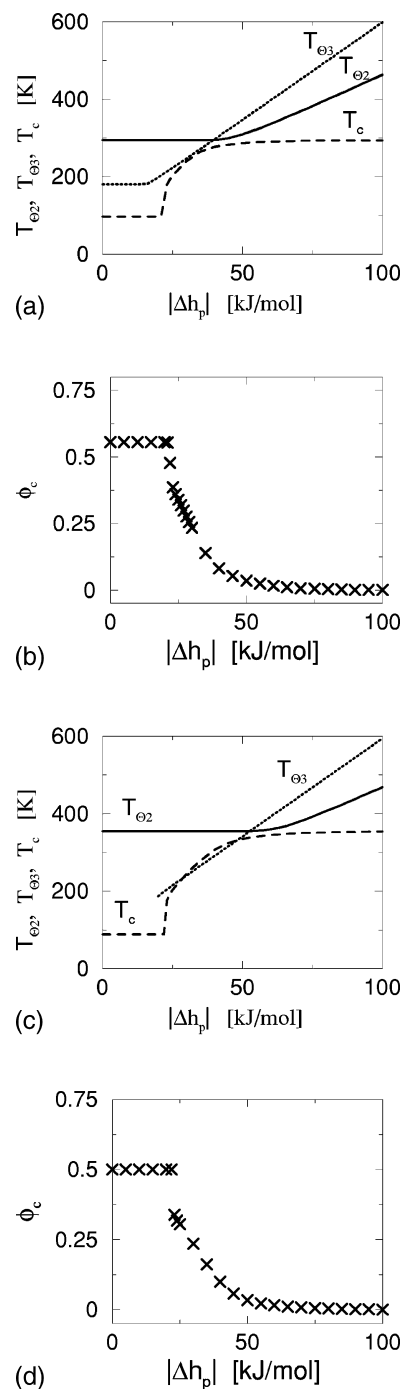


FIG. 7. (a) The characteristic temperatures of equilibrium polymerization solutions as functions of the energy of polymerization Δh_p and computed for the activated polymerization model described in the text. The temperatures considered include the critical temperature, the theta temperature $T_{\theta 2} \equiv T_{\theta}$, and the temperature $T_{\theta 3}$ where the third virial coefficient A_3 vanishes. (b) The critical composition φ_c as a function of Δh_p for the system analyzed in (c). Same as (a) but for a system with three-body interactions neglected ($\gamma=0$). (d) Same as (b) but for a system with three-body interactions neglected $\gamma=0$.

tions [see Eq. (2.22)] but also on the free energy parameters Δh_a and Δs_a governing the activation process for association. An example of this dependence is presented in Fig. 6 where the various curves correspond to different values of the activation entropy Δs_a , while the remaining parameters (Δh_p , Δs_p , Δh_a , ε_{FH}) are fixed to their former values. This figure demonstrates that the parameters describing the directional

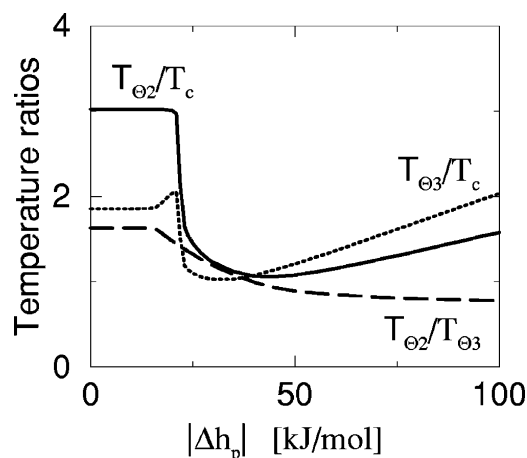


FIG. 8. Ratios of the characteristic temperatures of equilibrium polymer solutions as a function of the sticking energy Δh_p [see Fig. 7(a)].

interactions (Δh_p , Δs_p) and the isotropic contributions of the intermolecular potential (van der Waals or Flory interaction parameter χ) are insufficient to specify the magnitude of A_2 . The second virial coefficient also reflects the presence of many-body effects within the system, a point that Pitzer failed to appreciate and that is emphasized by Goldstein in his response to critical comments (by Singh and Pitzer¹¹²) regarding his assertion that many-body effects are largely responsible for deviations from the equation state properties of fluids.^{45,46} This problem potentially greatly complicates the determination of the second virial coefficient in strongly associating fluids and deserves a separate investigation. Note that the term “many-body effects” is defined here as physical factors, such as polarizability that strongly contribute to three-body interactions and thus to the effective two-body interactions.

We now consider the influence of the association energy Δh_p on the theta temperatures $T_{\Theta 2} \equiv T_{\Theta}$ and $T_{\Theta 3}$ in Fig. 7(a) when three-body interactions (at the monomer level) are included in the system's free energy. A curve for the critical temperature as function of the “sticking energy” $T_c(\Delta h_p)$ is also added for comparison. Inspection of Fig. 7(a) implies that (1) $T_{\Theta 2}$ exceeds $T_{\Theta 3}$ for systems exhibiting small (or zero) associative interactions, whereas the trend is opposite for solutions of strongly associating substances (i.e., with large $|\Delta h_p|$), and (2) the critical temperature T_c for phase separation never exceeds $T_{\Theta 2}$ or $T_{\Theta 3}$. The corresponding critical composition φ_c [see Fig. 7(b)] departs from the symmetrical value $\varphi_c=0.5$ that is typical for systems interacting exclusively with binary monomer-solvent potentials when $|\Delta h_p|$ is small or zero. Figure 7(c) analyzes the same quantities as in Fig. 7(a) for systems devoid of ternary interactions ($\gamma=0$) for comparison. The main difference between these two cases is the absence of a finite $T_{\Theta 3}$ for small $|\Delta h_p|$ and the relative location of the critical temperature and $T_{\Theta 3}$ in the intermediate coupling regime. As emphasized in Fig. 7(d), the critical composition φ_c for equilibrium polymer solutions with no ternary monomer-solvent interactions changes from $\varphi_c=0.5$ to values close to zero as the associative sticking energy $|\Delta h_p|$ grows infinitely. This behavior simply reflects the fact that the chains are becoming long at the critical point

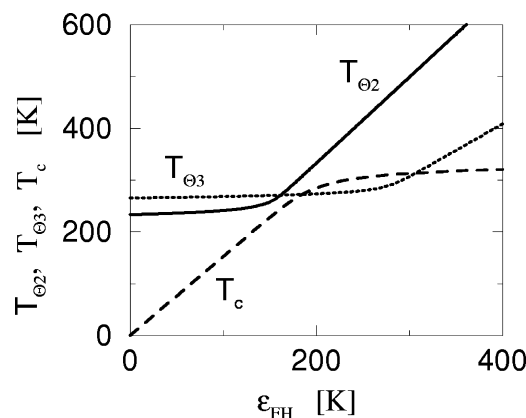


FIG. 9. The characteristic temperatures of equilibrium polymer solutions as a function of the exchange energy ϵ_{FH} and computed for the activated polymerization model described in the text. The temperatures considered include the critical temperature, the theta temperature $T_{\Theta 2} \equiv T_{\Theta}$, and the temperature $T_{\Theta 3}$ where the third virial A_3 coefficient vanishes.

for strong associative interactions, a feature well known for ordinary polymer solutions. Figure 8 supplements the information of Figs. 7(a) and 7(c) by showing the temperature ratios $T_{\Theta 2}/T_c$, $T_{\Theta 3}/T_c$, and $T_{\Theta 2}/T_{\Theta 3}$ as functions of $|\Delta h_p|$. All these ratios exhibit a plateau within the weak coupling regime, but then a decrease with increasing $|\Delta h_p|$, where two of these quantities ($T_{\Theta 2}/T_c$ and $T_{\Theta 3}/T_c$) pass through a minimum before displaying a further monotonic increase. The ratio $T_{\Theta 2}/T_{\Theta 3}$ diminishes monotonically with $|\Delta h_p|$. The occurrence of the small local maximum in $T_{\Theta 3}/T_c$ coincides with the end of the weak coupling regime.

While Figs. 7(a), 7(c), and 8 illustrate the variation of the characteristic temperatures of activated equilibrium polymerization and their ratios with $|\Delta h_p|$ at a fixed van der Waals interaction strength ϵ_{FH} , Figs. 9 and 10 examine how these properties depend on ϵ_{FH} when the associative interaction parameters remain unchanged. Figure 9 demonstrates that T_c varies linearly with ϵ_{FH} for an interaction range from zero to approximately 200 K and then approaches a plateau. In contrast, the theta temperatures $T_{\Theta 2}$ and $T_{\Theta 3}$ vary little with ϵ_{FH} until ϵ_{FH} exceeds certain “critical values” ($\epsilon_{FH}^{(cr)} \approx 150$ K for $T_{\Theta 2}$ and $\epsilon_{FH}^{(cr)} \approx 300$ K for $T_{\Theta 3}$). The increase of $T_{\Theta 3}$ with ϵ_{FH} is evidently delayed in comparison with that for $T_{\Theta 2}$. The characteristic temperature ratios $T_{\Theta 2}/T_c$ and $T_{\Theta 3}/T_c$ are plotted against ϵ_{FH} in Fig. 10, where they exhibit a minimum, while the variation of the ratio $T_{\Theta 2}/T_{\Theta 3}$ with ϵ_{FH} has a sigmoidal shape with a plateau at both small and large ϵ_{FH} .

F. Other metrics of fluid complexity

Two other basic measures of fluid complexity have been used before to quantify deviations from the law of corresponding states, the “solution compressibility factor” $Z_{II,c} \equiv \Pi v_{cell}/(kT_c \varphi_c)$ at the critical point and the rectilinear diameter A_d describing the degree to which the coexistence curve tilts (see Fig. 2). The osmotic compressibility factor $Z_{II,c}$ has been analyzed by us for a living polymerization model⁷⁵ and for the free association model used to describe the critical behavior of the Stockmayer fluid,¹¹³ a fluid where the particles are characterized by a Lennard-Jones (van der

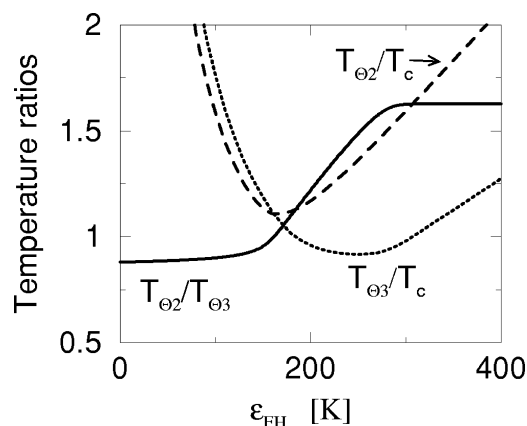


FIG. 10. Ratios of the characteristic temperatures of equilibrium polymer solutions that are analyzed in Fig. 9 as a function of the exchange energy ϵ_{FH} .

Waals) interaction with a point dipole interaction superimposed. Recently, Liu and Xiang³¹ and Xiang¹¹⁴ have advocated a generalized law of corresponding states where the difference $Z_{II,c} - Z_{II,c}^o$ (with the superscript o referring to simple fluids) replaces or augments the ω parameter of Pitzer's description.¹

The related ratio $\delta \equiv Z_{II,c}(\Delta h_p)/Z_{II,c}^o(\Delta h_p=0)$ is examined as a function of $|\Delta h_p|$ in Fig. 11 for the activated polymerization model when the ternary interactions are neglected for simplicity. In the weak coupling regime, the ratio δ is relatively constant, characteristic of the simple fluid behavior, while δ varies nonmonotonically in the intermediate coupling regime (as appreciable association at the critical point first begins to occur), first decreasing and then increasing toward a maximum as $|\Delta h_p|$ becomes larger. Finally, δ approaches zero for large $|\Delta h_p|$ in the strong coupling regime. The variation in Fig. 11 qualitatively resembles our previous finding for living polymerization⁷⁵ and can be used to determine the type of coupling between polymerization and phase separation. On the other hand, δ decreases monotonically with $|\Delta h_p|$ for the free association model,¹¹³ so that the trend in δ observed for the activated polymerization model is not universal. We now pass to other properties that can be used to quantify fluid complexity.

The shape of the phase boundaries in fluids undergoing equilibrium polymerization has been previously found by us^{12,72,74} to be quite sensitive to Δh_p and correspondingly to the extent of particle association Φ and the average size (polymer length L or the radius of gyration R_g) of the polymeric structures that form near the critical point.¹² Indeed, the importance of an understanding of this qualitative relation between the particle association and phase boundary asymmetry in fluid mixtures has been appreciated for a long time.¹¹⁵

The “law of the rectilinear diameter” expressed in Eq. (2.17) is one of the earliest discovered universal empirical relations describing the critical properties of fluids.^{19,79,80,82} Measurements for real fluids have not indicated appreciable deviations from this general relation outside the Ising critical region, except for a couple of cases where three-body interactions are especially large.^{45,46} As might be expected, the

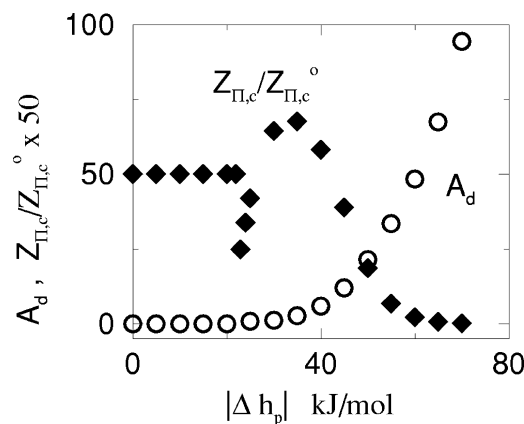


FIG. 11. The rectilinear diameter and the critical osmotic compressibility factor $Z_{II,c}$ (normalized by the corresponding quantity $Z_{II,c}^o$ for monomer-solvent systems) computed as functions of the polymerization energy $|\Delta h_p|$ for a solution exhibiting activated equilibrium polymerization. The free energy parameters are specified in the caption to Fig. 1, and the factor γ , describing the strength of ternary interactions, is set to zero (i.e., the ternary interactions are neglected in this illustrative example).

association of particles into large polymeric clusters with increasing association interaction tends to make A_d large. Hence, A_d is a sensitive measure of fluid complexity, as is the related acentric parameter ω .¹¹² This general trend toward asymmetric coexistence curves in simple and increasingly complex fluids (fluorocarbon, metallic, and salts) is nicely illustrated by Pitzer¹¹⁶ and is directly comparable to the trend predicted for the free association model with increasingly attractive associative interaction (compare inset of Fig. 1 from Ref. 12 to Fig. 1 of Pitzer¹¹⁶). Correspondingly, Fig. 11 presents A_d for the activated equilibrium polymerization model as a function of $|\Delta h_p|$ where the other free energy parameters are held fixed as in previous calculations discussed above, but ternary interactions are neglected for compatibility with the calculations of δ in the same figure. The magnitude of A_d increases monotonically and strongly with Δh_p , reflecting the increasing role of association on the phase separation boundary. This asymmetry in the coexistence curves of complex fluids is also captured by the acentric factor ω , explaining the previously observed strong correlation between ω and A_d .^{112,117} The highly sensitive nature of A_d to association and the disparity between the molecular shapes of solution components make this property a suitable metric for determining deviations from corresponding state scaling. Moreover, the determination of A_d does not rely on measurements close to the critical point (like Z_c), which tend to have greater experimental and theoretical uncertainty.

The experimental determination of ω and A_d necessarily relies on measurements in the two-phase region that are often time consuming, especially for complex fluids. Thus, it is useful to define physical quantities that provide essentially equivalent information but which refer to the *one-phase regime*. For over a hundred years, it has been known that there exists for diverse fluids a nearly linear locus of concentrations (density) and temperatures at which Z equals 1.^{90,117,118} This line of ideality ($Z=1$) is termed the “Boyle line” or the “Zeno line,” but we call it the “theta line” since it extrapolates to the theta temperature $T_{\Theta 2}$ as the concentration tends

toward zero. Hershbach and co-workers¹¹⁷ have shown that the slope k_Θ of the theta line correlates extremely well with the rectilinear diameter slope, and the reasons for the existence of this correlation are graphically illustrated in Ref. 117. (Basically, the rectilinear diameter curve roughly parallels the theta line.) Given this connection, it should not be surprising that Holleran¹¹⁸ has developed a generalized corresponding state description of fluids, based on the theta line and the slope k_Θ , which in turn provides a measure of deviation from simple fluid behavior. Because of the similarity of k_Θ and A_d , we do not pursue the explicit calculations of k_Θ here.

The definition of the theta line implies that k_Θ is rather large in simple fluids where $T_{\Theta 2}$ and T_c are well separated, but this slope must become progressively smaller as the strength Δh_p of the directional interparticle interactions increases, so that T_c approaches $T_{\Theta 2}$ [see Fig. 7(a)]. Additionally, Fig. 7(a) indicates that in the strong coupling regime, the gap between $T_{\Theta 2}$ and T_c opens up again, accompanying the inversion between $T_{\Theta 2}$ and $T_{\Theta 3}$, so that the slope k_Θ must increase again when Δh_p becomes very large.

The characteristic temperature ratios $T_{\Theta 2}/T_c$ and $T_{\Theta 3}/T_c$ are quite accessible from the experiment and should provide another useful measure of deviations from the simple fluid behavior. Recent simulations^{56,119} indicate, for instance, that the ratio $T_{\Theta 2}/T_c$ decreases (while ω correspondingly increases) as the relative strength of the anisotropic interactions [molecular shape anisotropy or the strength of a directional (quadrupolar) interaction] increases. The former trend is consistent with that illustrated in Fig. 8 for the intermediate coupling regimes, an interaction regime that should apply to many real fluids. Inglesias-Silva and Hall¹²⁰ have proposed a universal correlation relating $T_{\Theta 2}/T_c$ to ω in both polar and nonpolar fluids. The above temperature ratios are clearly of relevance for classifying fluid complexity, although these quantities do not seem to have been utilized for this purpose before.

IV. CORRESPONDING STATE DESCRIPTION OF ACTIVATED EQUILIBRIUM POLYMERIZATION

Having calculated a wide range of metrics for characterizing deviations from the simple fluid equation of state scaling, we now explore whether our theory, which is expressed in terms of microscopic interaction variables, can be recast in terms of these macroscopic observables. Such an approach directly follows the path pursued by van der Waals in developing the original two-parameter principle of corresponding states. As is clear from the previous section, this effort requires introducing extra reducing variables to describe complex fluids exhibiting association.

First, we mention existing generalized equations of state that address the influence of particle association on phase separation. The statistical associating fluid theories are based on the thermodynamic perturbation approach of Wertheim³⁹ and find widespread application in chemical engineering.^{40–43} Within these theories, the Helmholtz free energy of the fluids is decomposed into separate contributions describing the hard core repulsions of the molecules,

the van der Waals segmental interactions, and particle association, echoing the separability of van der Waals and complex fluid contributions to the compressibility factor Z , as assumed by Pitzer¹ in developing the generalized corresponding state description of fluids. This clean separation of contributions to the fluid's free energy is a consequence of the perturbative nature of Wertheim's theory and does not appear in our theory of associating fluids since the magnitude of the associative interaction need not necessarily be small.

Consider the Helmholtz free energy density of a fluid capable of undergoing both phase separation and self-assembly. To simplify matters, attention is initially confined to the FA model where no activation constraints act on the assembly process.⁷² The free energy density for this model can be written in a form that resembles that used for a simple binary mixture,¹¹³

$$f/(kT) = (1 - \varphi_1^o) \ln(1 - \varphi_1^o) + \varphi_1^o \ln[1 - \varphi_1^o(1 - \Phi)] + f_I, \quad (4.1a)$$

where the contribution arises from both the van der Waals and associative interactions and is given by

$$f_I = [\varphi_1^o(1 - \varphi_1^o)] \left[\frac{1}{2} - A_2 - \frac{[L(1 - \Phi) - 1]^2}{L(L - 1)\varphi_1^o(1 - \Phi)^2} \right] + \varphi_1^o \frac{L - 1}{L}, \quad (4.1b)$$

with φ_1^o being the initial monomer concentration, Φ denoting the extent of polymerization, and L designating the average cluster length (mass). Similarly, the "equation of state" of an associating fluid solution can be presented as

$$\frac{\Pi v_{\text{cell}}}{kT} = -\ln(1 - \varphi_1^o) - \varphi_1^o \frac{L - 1}{L} - (\varphi_1^o)^2 \left[\frac{1}{2} - A_2 - \frac{[L(1 - \Phi) - 1]^2}{L(L - 1)\varphi_1^o(1 - \Phi)^2} \right]. \quad (4.2)$$

Although it is apparent that the free energy is not separable into additive contributions, we can formally express $f/(kT)$ as a function of four dimensionless properties ($\varphi_1^o, A_2, \Phi, L$) of the polymerizing solution,

$$f/(kT) = \Psi(\varphi_1^o, A_2, \Phi, L), \quad (4.3)$$

where Ψ is a general scaling function for a particular class of fluids. Thus, an equation of state is obtained in terms of the concentration φ_1^o of the associating species, a measure of the phase stability with respect to phase separation, and the degree and spatial extent of polymerization that are specified by Φ and L , respectively. These last two quantities contain essential information about the free energy parameters governing the assembly process. Our analysis leading to Eq. (4.3) does not include the influence of ternary interactions, and the inclusion of these interactions into Eq. (4.3) requires the addition of the third virial coefficient A_3 to the list of scaling variables specifying f .

Theoretical studies of the critical properties of associating fluids introduce a formal Taylor expansion about the critical point, which naturally leads to the appearance of variables normalized with respect to their critical point values.

Thus, the free energy density of Eq. (4.3) can be formally expressed in terms of these new reduced variables,

$$f/(kT) = \Psi_r(\varphi_1^o/\varphi_c, A_2/A_{2c}, \Phi/\Phi_c, L/L_c), \quad \varphi_c \equiv (\varphi_1^o)_c, \quad (4.4)$$

where Ψ_r denotes a general scaling function of the reduced parameters. The ratio A_2/A_{2c} is temperature dependent, and its sensitivity to temperature is largely dictated by the distance between $T_{\Theta 2}$ (where A_2 vanishes) and the critical point (where Π becomes critically small, signaling thermodynamic instability). An expansion of A_2/A_{2c} in the variables T/T_c and $(T - T_{\Theta 2})/T_c$ leads to a dependence of $f/(kT)$ on five variables,

$$f/(kT) = \Psi'_r[\varphi_1^o/\varphi_c, T/T_c, (T - T_{\Theta 2})/T_c, \Phi/\Phi_c, L/L_c]. \quad (4.5)$$

The “'” on Ψ'_r serves to distinguish Ψ'_r from Ψ_r which is a function of four variables. Nonassociated fluids correspond to $\Phi \rightarrow 0$, $L \rightarrow 1$, and $T_{\Theta 2}/T_c \gg 1$, so that Eq. (4.5) simplifies to the classical equation of state,

$$f/(kT) = \Psi_r(\varphi_1^o/\varphi_c, T/T_c). \quad (4.6)$$

For fluids with weak interparticle associations, $\Phi \approx 0$ and $L \approx 1$, and Eq. (4.6) reduces to the form

$$f/(kT) = \Psi'_r[\varphi_1^o/\varphi_c, T/T_c, (T - T_{\Theta 2})/T_c]. \quad (4.7)$$

Since $T_{\Theta 2}/T_c$ can be generally related to the rectilinear diameter A_d , the acentric factor ω and the slope k_Θ of the theta line, Eq. (4.7) recovers the scaling relation suggested in the limit of weak associative interactions by Pitzer,

$$f/(kT) \approx \Psi_r(\varphi_1^o/\varphi_c, T/T_c, \omega). \quad (4.8)$$

The generalized equation of state [Eq. (4.5)] also simplifies under conditions where the polymeric structures are *permanent*, i.e., $\Phi \approx 1$. In this case, $f/(kT)$ again reduces to Eq. (4.7) since L is directly related to $T_{\Theta 2}/T_c$ in ordinary polymer solutions.^{66,67} A more refined analysis for polymer solutions requires the incorporation of three-body interactions and fluctuation effects beyond the mean field theory.^{70,71}

V. DISCUSSION

The corresponding state description of fluids is based on a general dimensional analysis of the thermodynamic properties of fluids and predicts that all thermodynamic properties of all “simple” fluids, interacting with common potential, obey the *same functional form* when the temperature and density are reduced by their critical point values.^{1,13,15} Predicting and designing fluid properties based on the classical equation of state are now routine in materials engineering, despite the well-known existence of significant deviations from “universality” for fluids having complex interactions. Although it is unclear whether a universal reduced variable description exists for “complex” fluids whose interactions involve multiple energy and spatial scales, some deviations from a simple equation of state can be described (according to Pitzer) through the introduction of a single additional reducing variable, Pitzer’s “acentric factor” ω , which has become a fundamental quantity in the engineering description of fluids.^{1,18,112} The success of this parametric treatment of

fluid properties provides some encouragement for future studies of the *existence* of a generalized corresponding state for complex fluids. More recently, other thermodynamic parameters besides ω have been introduced in an attempt to develop a generalized equation of state of complex fluids. These extra parameters have been identified as measures of particle association,²⁶ as well as measures of the strength of *many-body* interactions.^{45,46} If a generalized state description exists, it is now clear, however, that the complexity of this treatment must surpass that of the correlations introduced by Pitzer.¹

The present work seeks to develop an understanding of corresponding state scaling by examining the statistical thermodynamics of a representative model complex fluid (activated equilibrium polymerization solution) that exhibits both molecular association and the effects of many-body interactions. In particular, our calculations of critical properties (T_c, φ_c) and equation of state properties ($A_2, A_3, T_{\Theta 2}, T_{\Theta 3}$) are analyzed in a manner that parallels the procedure followed by van der Waals for simple fluids. These calculations indicate that $T_{\Theta 3}$ can indeed exceed $T_{\Theta 2}$, in qualitative accord with de Gennes’ *m*-cluster model⁸⁹ and with the interpretation of the polyelectrolyte data that is described in Sec. III. The inversion from the “normal” behavior of simple fluids (A_2 vanishing before A_3 upon reducing solvent quality) emerges from our calculations only when the associative interactions are relatively strong (i.e., within the intermediate or strong coupling regimes) and only when the monomer activation process proceeds upon cooling. However, the polymers that form in these associating fluids cannot be swollen under phase separation conditions, as suggested by de Gennes, but rather are the result of clustering occurring in the *one-phase region*. Dynamic clustering cannot be equated with phase separation, although experimentally it is easy to confuse these two phenomena with each other. Our analysis not only delineates a thermodynamic phenomenon that is absent in simple fluids, but this singular pattern of self-assembly apparently provides a good opportunity to recognize strongly associating fluids, a first step in quantifying the interactions in these systems.

While the existence of a generalized corresponding state description for all fluids remains an open question, it is clearly useful to introduce thermodynamic metrics that determine the relative complexity of a given fluid. These metrics should aid in establishing generalized equations of state that at least apply to restricted classes of fluids defined by the metric. The theta temperatures ($T_{\Theta 2}, T_{\Theta 3}$) associated with the vanishing of the second and third virial coefficients, respectively, along with the critical temperature T_c for phase separation, provide valuable information concerning fluid complexity. Similar information is obtained from the acentric factor ω of Pitzer,¹ the rectilinear diameter A_d (describing the anisotropy of the phase boundary), the reduced pressure at the critical point, the critical compressibility factor, and the slope k_Θ of the “theta line” where $Z=1$. The metrical parameters describing fluid complexity are also found to exhibit an appreciable dependence on many-body interactions, a phenomenon that complicates the determination of virial coefficients.

ACKNOWLEDGMENTS

We thank Ferenc Horkay of NIH for many helpful discussions relating to the polyelectrolyte data shown in Fig. 5(a) and for providing these data in the new representation shown in Fig. 5(b). This research is supported, in part, by NSF Grant No. CHE-0416017.

APPENDIX A: ROLE OF TERNARY INTERACTIONS IN THE THERMODYNAMICS OF MONOMER-SOLVENT SYSTEMS IN THE ABSENCE OF POLYMERIZATION

The Flory-Huggins-type free energy of mixing Δf^{mix} for an incompressible mixture composed of monomers and (one bead) solvent molecules that interact exclusively through two-body potentials is conventionally expressed in terms of the interaction parameter $\chi_o = \varepsilon_{\text{FH}}/T$ and the monomer volume fraction φ as

$$\frac{\Delta f^{\text{mix}}}{kT} = \varphi \ln \varphi + (1 - \varphi) \ln(1 - \varphi) + \varphi(1 - \varphi)\chi_o, \quad (\text{A1})$$

where T is the absolute temperature, k denotes the Boltzmann constant, and $\varepsilon_{\text{FH}} = \varepsilon_{mm} + \varepsilon_{ss} - 2\varepsilon_{ms}$ is the exchange energy with the subscripts mm , ss , and ms labeling all three possible pairs of interacting monomers (m) and solvent (s) species and with $\{\varepsilon_{\alpha\beta}\}$ designating the microscopic van der Waals energies. If the microscopic self-interaction energies are taken as the energy zero ($\varepsilon_{mm} = \varepsilon_{ss} = 0$), Eq. (A1) also describes the specific Helmholtz free energy of the mixture.

The inclusion of ternary (three-body) interactions converts Eq. (A1) into the relation

$$\frac{\Delta f^{\text{mix}}}{kT} = \varphi \ln \varphi + (1 - \varphi) \ln(1 - \varphi) + \varphi(1 - \varphi) \times [\chi_o + \chi_{mms}\varphi + \chi_{mss}(1 - \varphi)], \quad (\text{A2})$$

where the two extra terms $\varphi^2(1 - \varphi)\chi_{mms}$ and $\varphi(1 - \varphi)^2\chi_{mss}$ quantify the strengths of ternary interactions within monomer-monomer-solvent (mms) and monomer-solvent-solvent (mss) triads, respectively. The form of Eq. (A2) coincides with that derived from the simplified lattice cluster theory (SLCT) for binary polymer blends when the polymerization indices of the two structured monomer blend species are set to unity in the expression for the combinatorial part of the free energy Δf^{mix} from Ref. 50. Our SLCT analysis for binary polymer blends also indicates that both χ_{mms} and χ_{mss} of Eq. (A2) should be proportional to the exchange energy ε_{FH} when only terms linear in $1/T$ are considered. Consequently, we can write $\chi_{mms} = \alpha_2 \varepsilon_{\text{FH}}/T \equiv \varepsilon_2/T$ and $\chi_{mss} = \alpha_3 \varepsilon_{\text{FH}}/T \equiv \varepsilon_3/T$, where $\varepsilon_2 \equiv \alpha_2 \varepsilon_{\text{FH}}$ and $\varepsilon_3 \equiv \alpha_3 \varepsilon_{\text{FH}}$.

The effective (small angle neutron scattering) parameter χ_{eff} in the incompressible limit is defined in terms of the free energy of mixing Δf^{mix} by

$$\frac{\partial^2(\Delta f^{\text{mix}}/kT)}{\partial \varphi^2} = \frac{1}{\varphi} + \frac{1}{1 - \varphi} - 2\chi_{\text{eff}} \quad (\text{A3})$$

and is evaluated by taking the derivative of Δf^{mix} from

Eq. (A2). While χ_{eff} for a system with exclusively binary interactions ($\chi_{\text{eff}} = \chi_o = \varepsilon_{\text{FH}}/T$) is composition independent, the inclusion of three-body interactions implies that χ_{eff} becomes a polynomial in φ ,

$$\chi_{\text{eff}} = b/T + \varphi c/T, \quad b \equiv \varepsilon_{\text{FH}} - \varepsilon_2 + 2\varepsilon_3, \quad c \equiv 3(\varepsilon_2 - \varepsilon_3). \quad (\text{A4})$$

The critical composition φ_c for the phase separation is determined by the condition $\partial^3 \Delta f^{\text{mix}} / \partial \varphi^3|_{\varphi=\varphi_c} = 0$, which yields

$$\varphi_c = \frac{\sqrt{b^2 + c^2 + bc} - b + c}{3c}, \quad (\text{A5})$$

whereas the critical temperature is computed from the stability condition obtained by setting Eq. (A3) to zero and inserting the expression for φ_c from Eq. (A5) into the resulting equation, giving

$$T_c = 2(b + c\varphi_c)\varphi_c(1 - \varphi_c). \quad (\text{A6})$$

The critical osmotic compressibility factor $Z_{\text{II},c}$ then equals

$$Z_{\text{II},c} = \frac{\Pi_c v_{\text{cell}}}{kT_c \varphi_c} = -\frac{1}{\varphi_c} \ln(1 - \varphi_c) - \frac{1}{1 - \varphi_c} \frac{b + (2/3)c\varphi_c}{b + c\varphi_c}, \quad (\text{A7})$$

where Π_c denotes the osmotic pressure at the critical point. Note that $Z_{\text{II},c}$ depends only on b and c [see Eq. (A5)].

Next, we continue considering basic properties related to the osmotic pressure. Since either monomers or solvent molecules can be the minority species, there are two osmotic virial expansions and two osmotic pressures, say, Π_m and Π_s , where the subscripts m and s denote the majority and minor species, respectively. The virial series are generated from Eq. (A1) by evaluating the chemical potentials μ_m and μ_s and by expanding the logarithmic term about the limiting vanishing volume fractions,

$$\frac{\Pi_m v_{\text{cell}}}{kT} = -\frac{\mu_m}{kT} = A_1^{(m)}(1 - \varphi) + A_2^{(m)}(1 - \varphi)^2 + A_3^{(m)}(1 - \varphi)^3 + \cdots, \quad (1 - \varphi) \approx 0 \quad (\text{A8})$$

and

$$\frac{\Pi_s v_{\text{cell}}}{kT} = -\frac{\mu_s}{kT} = A_1^{(s)}\varphi + A_2^{(s)}\varphi^2 + A_3^{(s)}\varphi^3 + \cdots, \quad \varphi \approx 0, \quad (\text{A9})$$

where the volume v_{cell} is the average volume of a monomer and a solvent molecule and where $A_1^{(\alpha)}$, $A_2^{(\alpha)}$, and $A_3^{(\alpha)}$, $\alpha = m, s$, are the first, second, and third virial coefficients, respectively, which are given by

$$A_1^{(m)} = A_1^{(s)} = 1, \quad (\text{A10})$$

$$A_2^{(m)} = \frac{1}{2} - \frac{b + c}{T}, \quad A_2^{(s)} = \frac{1}{2} - \frac{b}{T}, \quad (\text{A11})$$

$$A_3^{(m)} = \frac{1}{3} + \frac{2c}{3T}, \quad A_3^{(s)} = \frac{1}{3} - \frac{2c}{3T}, \quad (\text{A12})$$

with b and c defined by Eq. (A4). The corresponding theta temperatures $T_{\Theta}^{(m)}$ and $T_{\Theta}^{(s)}$ are defined as the temperatures at which the second virial coefficients $A_2^{(m)}$ and $A_2^{(s)}$ vanish, respectively. Thus, we have

$$T_{\Theta}^{(m)} \equiv T_{\Theta_2}^{(m)} = 2(b+c), \quad T_{\Theta}^{(s)} \equiv T_{\Theta_2}^{(s)} = 2b. \quad (\text{A13})$$

APPENDIX B: POLYMER BLENDS: ANOTHER CLASS OF COMPLEX MIXTURES

The present appendix demonstrates that a similar corresponding state description to that derived in Sec. III for equilibrium polymerization solutions also applies to polymer blends. The monomer-solvent system described in Appendix A is a limiting case of binary polymer blends. In particular, we seek to reformulate the blend free energy of mixing density Δf^{mix} (that is expressed commonly as a function of microscopic interaction parameters) in terms of macroscopic observables. Our recent statistical thermodynamical analysis of incompressible binary polymer blends^{49,50} indicates that Δf^{mix} takes the following form:

$$\frac{\Delta f^{\text{mix}}}{kT} = \frac{\varphi}{M} \ln \varphi + \frac{(1-\varphi)}{M\lambda} \ln(1-\varphi) + \varphi(1-\varphi) \left[a + \frac{b + (1/3)c + (1/3)c\varphi}{T} \right], \quad (\text{B1})$$

where $\varphi \equiv \varphi_1 = 1 - \varphi_2$ is the volume fraction of component 1, $M \equiv M_1$ is the number of united atom groups in a single chain of blend species 1, $\lambda = M_2/M_1$, and b and c are the coefficients determining the small angle neutron scattering χ parameter (expressed as an interaction parameter between united atom groups) $\chi = a + (b+c\varphi)/T$. All these three coefficients are functions of monomer molecular structure, while b and c depend in addition to the exchange interaction energy ϵ_{FH} .^{49,50}

Since either component of a binary blend can be the dilute species, there are two osmotic virial expansions and consequently two sets of osmotic virial coefficients A_2 and A_3 , namely, $A_2^{(1)}$, $A_3^{(1)}$ and $A_2^{(2)}$, $A_3^{(2)}$ where superscripts 1 and 2 denote the majority species. As described in our prior paper,⁴⁹ these osmotic virial coefficients are given by

$$A_2^{(1)} = \frac{1}{2} - \left(a + \frac{b+c}{T} \right) M_1, \quad A_3^{(1)} = \frac{1}{3} + \frac{2c}{3T} M_1 \quad (\text{B2})$$

and

$$A_2^{(2)} = \frac{1}{2} - \left(a + \frac{b}{T} \right) M_2, \quad A_3^{(2)} = \frac{1}{3} - \frac{2c}{3T} M_2. \quad (\text{B3})$$

The relevance of Eqs. (B2) and (B3) lies not only in the possibility of evaluating $A_2^{(i)}$ and $A_3^{(i)}$ ($i=1,2$) based on the geometrical indices characterizing monomer molecular structures of the two blend components^{49,50} but also in the opportunity of determining the combinations of coefficients a , b , and c [that enter Eq. (B1)] from a knowledge of the second

and third virial coefficients. Thus, Eq. (B1) can be rewritten as

$$\frac{\Delta f^{\text{mix}}}{kT} = \frac{1}{M} \left[\varphi \ln \varphi + \frac{1-\varphi}{\lambda} \ln(1-\varphi) + \varphi(1-\varphi)(1/6) \times [5 - \varphi - 6A_2^{(1)} - 3A_3^{(1)}(2-\varphi)] \right] \quad (\text{B4})$$

or

$$\frac{\Delta f^{\text{mix}}}{kt} = \frac{1}{\lambda M} [\lambda \varphi \ln \varphi + (1-\varphi) \ln(1-\varphi) + \varphi(1-\varphi)(1/6) \times [4 + \varphi - 6A_2^{(2)} - 3A_3^{(2)}(1+\varphi)]] \quad (\text{B5})$$

The virial coefficients in Eqs. (B4) and (B5) correspond to the cases in which species 1 and 2 are the majority components, respectively. Expressions (B4) and (B5) provide a basis for the corresponding state description of binary polymer blends.

¹K. S. Pitzer, J. Am. Chem. Soc. **77**, 3427 (1955); K. S. Pitzer, D. Z. Lippmann, R. F. Curl, C. M. Huggins, and D. E. Petersen, *ibid.* **77**, 3433 (1955).

²The LJ potential is specified by only *two* molecular parameters, an energy well depth ϵ and an interaction range σ .

³K. Van Workum and J. F. Douglas, Phys. Rev. E **71**, 031502 (2005); **73**, 031502 (2006). See earlier references cited in these papers.

⁴L. Boltzmann, *Lectures in Gas Theory* (University of California Press, Berkeley, 1964), Pt. II, Chap. 6; see also K. Olaussen and G. Stell, J. Stat. Phys. **62**, 221 (1991).

⁵M. Wertheim, J. Chem. Phys. **85**, 2929 (1986).

⁶G. Jackson, W. G. Chapman, and K. E. Gubbins, Mol. Phys. **65**, 1 (1988).

⁷F. Sciortino, E. Bianchi, J. F. Douglas, and P. Tartaglia, J. Chem. Phys. **126**, 194903 (2007).

⁸F. Sciortino, S. Mossa, E. Zaccarelli, and P. Tartaglia, Phys. Rev. Lett. **93**, 055701 (2004).

⁹S. Salaniwal, S. K. Kumar, and A. Z. Panagiotopoulos, Langmuir **19**, 5164 (2003).

¹⁰W. van Ketel, C. Das, and D. Frenkel, Phys. Rev. Lett. **94**, 135703 (2005).

¹¹M. Sedlak, J. Phys. Chem. B **110**, 4329 (2006); **110**, 4339 (2006).

¹²K. Rah, K. F. Freed, J. Dudowicz, and J. F. Douglas, J. Chem. Phys. **124**, 144906 (2006).

¹³J. L. Sengers, *How Fluids Unmix: Discoveries by the School of van der Waals and Kamerlingh Onnes* (Koninklijke Akademie van Wetenschappen, Amsterdam, 2002).

¹⁴T. W. Leyland, Jr. and P. S. Chapple, Ind. Eng. Chem. **60**, 15 (1968).

¹⁵J. H. van der Waals, Dissertation, University of Leiden, 1873. See Ref. **13** for discussion.

¹⁶J. Kestin, S. T. Ro, and W. A. Wakeham, Physica (Amsterdam) **58**, 165 (1972); J. Kestin, H. E. Khalifa, S. T. Ro, and W. A. Wakeham, Physica A **88**, 242 (1977).

¹⁷J. de Boer and A. Michels, Physica (The Hague) **5**, 945 (1938).

¹⁸K. S. Pitzer, J. Chem. Phys. **7**, 583 (1939).

¹⁹E. A. Guggenheim, J. Chem. Phys. **13**, 253 (1945).

²⁰J. de Boer, Physica (Amsterdam) **14**, 510 (1948); **14**, 520 (1948).

²¹H. E. Stanley, *Introduction to Phase Transitions and Critical Phenomena* (Oxford University Press, New York, 1971).

²²P.-G. de Gennes, *Scaling Concepts in Polymer Physics* (Cornell University Press, Ithaca, NY, 1979).

²³A similar and more direct implementation of this idea has recently been adopted by M. G. Noro and D. Frenkel, J. Chem. Phys. **113**, 2941 (2000).

²⁴J. O. Hirschfelder, F. T. McClure, and I. F. Weeks, J. Chem. Phys. **10**, 201 (1942).

²⁵R. E. Leckenby and E. J. Robbins, Proc. R. Soc. London, Ser. A **291**, 389 (1966).

²⁶W. M. Kalback and K. E. Starling, Proc. Okla. Acad. Sci. **56**, 125 (1976).

²⁷K. S. Pitzer and R. F. Curl, J. Am. Chem. Soc. **79**, 2369 (1957).

²⁸P. L. Cheuh and J. M. Prausnitz, AIChE J. **13**, 897 (1967).

- ²⁹ C. Tsonopoulos, *AIChE J.* **20**, 263 (1974).
- ³⁰ H. Orbrej and J. H. Vera, *AIChE J.* **29**, 107 (1983).
- ³¹ D. X. Liu and H. W. Xiang, *Int. J. Thermophys.* **24**, 1667 (2003).
- ³² W. H. Thompson, Thesis, Penn State University, 1966.
- ³³ D.-Y. Peng and L. I. Stiel, *AIChE J.* **17**, 1008 (1971); T. P. Eubank and J. M. Smith, *ibid.* **8**, 117 (1962).
- ³⁴ F. Dolezalek, *Z. Phys. Chem., Stoechiom. Verwandtschaftsl.* **64**, 727 (1908); **83**, 45 (1913).
- ³⁵ J. J. van Laar, *Proc. K. Acad. Wetensch Amsterdam* **7**, 517 (1905); **10**, 45 (1913).
- ³⁶ J. H. Hildebrand and R. L. Scott, *The Solubility of Non-Electrolytes* (Reinhold, New York, 1950), Chap. 11.
- ³⁷ R. L. Scott, *J. Phys. Chem.* **69**, 261 (1965); R. L. Scott, *Acc. Chem. Res.* **20**, 97 (1987).
- ³⁸ J. C. Wheeler, S. J. Kennedy, and P. Pfeuty, *Phys. Rev. Lett.* **45**, 1748 (1980); J. C. Wheeler and P. Pfeuty, *Phys. Rev. A* **24**, 1050 (1981); *J. Chem. Phys.* **74**, 6415 (1981); *Phys. Rev. Lett.* **46**, 1409 (1981); J. C. Wheeler, *ibid.* **53**, 174 (1984); S. J. Kennedy and J. C. Wheeler, *J. Chem. Phys.* **78**, 1523 (1983); **78**, 953 (1983); **88**, 1040 (1984).
- ³⁹ M. S. Wertheim, *J. Stat. Phys.* **35**, 19 (1984); **35**, 35 (1984); **42**, 459 (1986); **42**, 477 (1986).
- ⁴⁰ I. E. Economou and M. D. Donohue, *AIChE J.* **37**, 1875 (1991).
- ⁴¹ S. H. Huang and M. Radosz, *Ind. Eng. Chem. Res.* **30**, 1994 (1991).
- ⁴² J. Gross and G. Sadowski, *Ind. Eng. Chem. Res.* **40**, 1244 (2001).
- ⁴³ S. B. Kiselev, J. F. Ely, H. Adidharma, and M. Radosz, *Fluid Phase Equilib.* **183-184**, 53 (2001).
- ⁴⁴ P. H. Van Konynenberg and R. L. Scott, *Philos. Trans. R. Soc. London, Ser. A* **298**, 495 (1980).
- ⁴⁵ R. E. Goldstein and N. W. Ashcroft, *Phys. Rev. Lett.* **55**, 2164 (1985); R. E. Goldstein, A. Parola, N. W. Ashcroft, M. W. Pestak, M. H. W. Chan, J. R. de Bruyn, and D. A. Balzarini, *ibid.* **58**, 41 (1987); M. W. Pestak, R. E. Goldstein, M. H. W. Chan, J. R. de Bruyn, D. A. Balzarini, and N. W. Ashcroft, *Phys. Rev. B* **36**, 599 (1987).
- ⁴⁶ J. R. de Bruyn and R. E. Goldstein, *J. Chem. Phys.* **95**, 9424 (1991).
- ⁴⁷ H. J. C. Berendsen, R. E. Grigera, and T. P. Straatsma, *J. Phys. Chem.* **91**, 6269 (1987).
- ⁴⁸ T. A. Orofino and P. J. Flory, *J. Chem. Phys.* **26**, 1067 (1957); see also B. J. Cherayil, J. F. Douglas, and K. F. Freed, *ibid.* **83**, 5293 (1985); **87**, 3089 (1987).
- ⁴⁹ J. Dudowicz, K. F. Freed, and J. F. Douglas, *J. Chem. Phys.* **116**, 9983 (2002).
- ⁵⁰ J. Dudowicz, K. F. Freed, and J. F. Douglas, *Phys. Rev. Lett.* **88**, 095503 (2002).
- ⁵¹ D. Frenkel and A. A. Louis, *Phys. Rev. Lett.* **68**, 3363 (1992); M. Dijkstra and D. Frenkel, *ibid.* **68**, 3363 (1992).
- ⁵² H. Yamakawa, *Modern Theory of Polymer Solutions* (Harper and Row, New York, 1971).
- ⁵³ K. F. Freed, *Renormalization Group Theory of Macromolecules* (Wiley, New York, 1987).
- ⁵⁴ Y. Nakamura, T. Norisuye, and A. Teramoto, *Macromolecules* **24**, 4904 (1991); Y. Nakamura, K. Akasaka, K. Katayama, T. Norisuye, and A. Teramoto, *ibid.* **25**, 1134 (1992); Y. Nakamura, N. Inoue, T. Norisuye, and A. Teramoto, *ibid.* **30**, 631 (1997).
- ⁵⁵ J. Li, Y. Wan, X. Xu, and J. W. Mays, *Macromolecules* **28**, 5347 (1995).
- ⁵⁶ G. MacDowell, C. Menduiña, C. Vega, and E. de Miguel, *Phys. Chem. Chem. Phys.* **5**, 2851 (2003).
- ⁵⁷ T. Norisuye and H. Fujita, *Macromol. Chem. Phys.* **2**, 293 (1991).
- ⁵⁸ I. Progogine, A. Bellemans, and C. Naar-Colin, *J. Chem. Phys.* **26**, 751 (1957).
- ⁵⁹ P. J. Flory, R. A. Orwoll, and A. Vrij, *J. Am. Chem. Soc.* **86**, 3507 (1964); **86**, 3515 (1964).
- ⁶⁰ V. S. Nanda and R. Simha, *J. Chem. Phys.* **41**, 3870 (1964).
- ⁶¹ I. C. Sanchez and R. H. Lacombe, *J. Phys. Chem.* **80**, 2352 (1976).
- ⁶² R. Dickman and C. K. Hall, *J. Chem. Phys.* **85**, 4108 (1986); **89**, 3108 (1988).
- ⁶³ J. Dudowicz and K. F. Freed, *Macromolecules* **28**, 6625 (1995).
- ⁶⁴ K. S. Schweizer and J. G. Curro, *J. Chem. Phys.* **89**, 3350 (1988).
- ⁶⁵ J. Cheng and S. I. Sandler, *Chem. Eng. Sci.* **49**, 2277 (1994); R. J. Sadus, *J. Phys. Chem.* **99**, 12363 (1995).
- ⁶⁶ M. Daoud and G. Jannik, *J. Phys. (Paris)* **37**, 973 (1976).
- ⁶⁷ I. C. Sanchez, *J. Appl. Phys.* **58**, 2871 (1985).
- ⁶⁸ B. Chu and Z. Wang, *Macromolecules* **21**, 2283 (1988).
- ⁶⁹ M. Muthukumar, *J. Chem. Phys.* **85**, 4722 (1997).
- ⁷⁰ M. A. Anisimov, A. F. Kostko, J. V. Sengers, and I. K. Yudin, *J. Chem. Phys.* **123**, 164901 (2005).
- ⁷¹ M. A. Anisimov and J. V. Sengers, *Mol. Phys.* **103**, 3061 (2005); J. S. Hager, M. A. Anisimov, J. V. Sengers, and E. E. Gorodetskii, *J. Chem. Phys.* **117**, 5940 (2002); M. A. Anisimov, V. A. Agayan, and E. E. Gorodetskii, *JETP Lett.* **72**, 578 (2000).
- ⁷² J. Dudowicz, K. F. Freed, and J. F. Douglas, *J. Chem. Phys.* **119**, 12645 (2003).
- ⁷³ J. Dudowicz, K. F. Freed, and J. F. Douglas, *J. Chem. Phys.* **111**, 7116 (1999).
- ⁷⁴ J. Dudowicz, K. F. Freed, and J. F. Douglas, *J. Chem. Phys.* **112**, 1002 (2000).
- ⁷⁵ J. Dudowicz, K. F. Freed, and J. F. Douglas, *J. Chem. Phys.* **113**, 434 (2000).
- ⁷⁶ A. Anderko, *Fluid Phase Equilib.* **45**, 39 (1989).
- ⁷⁷ L. Cailletet and E. Mathias, *C. R. Hebd. Seances Acad. Sci.* **102**, 1202 (1886); **104**, 1663 (1887).
- ⁷⁸ J. A. Zollweg and G. W. Mulholland, *J. Chem. Phys.* **57**, 1021 (1972).
- ⁷⁹ See Eq. (6.3) of Ref. 19.
- ⁸⁰ J. S. Rowlinson, *Nature (London)* **319**, 362 (1986).
- ⁸¹ J. W. Wang and M. A. Anisimov, *Phys. Rev. E* **75**, 051107 (2007).
- ⁸² J. F. Douglas and T. Ishinabe, *Phys. Rev. E* **51**, 1791 (1995); see numerous references describing the influence of fluctuations on the calculated critical temperature.
- ⁸³ M. A. Anisimov and J. W. Wang, *Phys. Rev. Lett.* **97**, 025703 (2006); C. N. Yang and T. D. Lee, *Phys. Rev.* **87**, 404 (1952); T. D. Lee and C. N. Yang, *ibid.* **87**, 410 (1952); A. D. Bruce and N. B. Wilding, *Phys. Rev. Lett.* **68**, 193 (1992).
- ⁸⁴ H. Wennerström and B. Lindman, *Phys. Rep.* **52**, 1 (1979); see Fig. 1.3; A. Floriano, E. Caponetti, and A. Z. Panagiotopoulos, *Langmuir* **15**, 3143 (1999); A. Z. Panagiotopoulos, A. Floriano, and S. K. Kumar, *ibid.* **18**, 2940 (2002).
- ⁸⁵ S. K. Kumar and A. Z. Panagiotopoulos, *Phys. Rev. Lett.* **82**, 5060 (1999); S. K. Kumar and J. F. Douglas, *ibid.* **87**, 188301 (2001).
- ⁸⁶ A. Mourchid, A. Delville, J. Lambard, E. Lecoliers, and P. A. Levitz, *Langmuir* **11**, 1942 (1995).
- ⁸⁷ (a) F. Horkay, I. Tasaki, and P. J. Basser, *Biomacromolecules* **1**, 84 (2000); (b) **2**, 195 (2001); (c) F. Horkay, P. J. Basser, A. Hecht, and E. Geissler, *Macromolecules* **33**, 8329 (2000); (d) F. Horkay, A. Hecht, P. J. Basser, and E. Geissler, *ibid.* **34**, 4285 (2001).
- ⁸⁸ Observations for DNA and SPS solutions (Ref. 97) are concluded from the unpublished data of Horkay, but the results are quite similar to those obtained for the polyacrylate gels that are described in Ref. 87.
- ⁸⁹ P. G. de Gennes, *C. R. Acad. Sci., Ser. II: Mec., Phys., Chim., Sci. Terre Univers* **313**, 1117 (1991); *Pure Appl. Chem.* **64**, 1585 (1992).
- ⁹⁰ J. G. Poyles, *J. Phys. C* **16**, 503 (1983).
- ⁹¹ K. Huber, *Macromolecules* **97**, 9825 (1993).
- ⁹² F. Horkay and P. J. Basser, *Biomacromolecules* **5**, 232 (2004).
- ⁹³ S. C. Lin, W. I. Lee, and J. M. Schurr, *Biopolymers* **17**, 1041 (1978).
- ⁹⁴ K. S. Schmitz, M. Lu, and J. Gauntt, *J. Chem. Phys.* **78**, 5059 (1983).
- ⁹⁵ M. Sedlak and E. J. Amis, *J. Chem. Phys.* **96**, 817 (1992).
- ⁹⁶ J. J. Tanahatoo and M. E. Kuil, *J. Phys. Chem. B* **101**, 10839 (1997).
- ⁹⁷ B. D. Ermi and E. J. Amis, *Macromolecules* **31**, 7378 (1998).
- ⁹⁸ Y. Zhang, J. F. Douglas, B. D. Ermi, and E. J. Amis, *J. Chem. Phys.* **114**, 3299 (2001).
- ⁹⁹ F. W. Starr, J. F. Douglas, and S. C. Glotzer, *J. Chem. Phys.* **119**, 1777 (2003).
- ¹⁰⁰ S. Jungst, B. Knuth, and F. Hensel, *Phys. Rev. Lett.* **55**, 2160 (1985).
- ¹⁰¹ P. J. Flory and J. E. Osterheld, *J. Phys. Chem.* **58**, 653 (1954).
- ¹⁰² M. A. Y. Axelos, M. M. Mestdag, and J. Francois, *Macromolecules* **27**, 6594 (1994).
- ¹⁰³ E. Raspaud, M. Olvera de la Cruz, J.-L. Sikoravs, and F. Livolant, *Biophys. J.* **74**, 381 (1984).
- ¹⁰⁴ P. J. Flory, *J. Chem. Phys.* **21**, 162 (1953).
- ¹⁰⁵ P. B. Warren, *J. Phys. II* **7**, 343 (1997).
- ¹⁰⁶ M. Olvera de la Cruz, L. Belloni, M. Delsanti, J. P. Dalbiez, O. Spalla, and M. Drifford, *J. Chem. Phys.* **103**, 5781 (1995).
- ¹⁰⁷ M. Muthukumar, *Macromolecules* **35**, 9142 (2002).
- ¹⁰⁸ M. Romero-Enrique, G. Orkoulas, A. Z. Panagiotopoulos, and M. E. Fisher, *Phys. Rev. Lett.* **85**, 4558 (2000).
- ¹⁰⁹ Q. L. Yan and J. J. DePablo, *Phys. Rev. Lett.* **88**, 095504 (2002).
- ¹¹⁰ Q. L. Yan and J. J. DePablo, *J. Chem. Phys.* **114**, 1727 (2001).
- ¹¹¹ J. C. Shelley and G. N. Patey, *J. Chem. Phys.* **103**, 8299 (1995).
- ¹¹² R. Singh and K. S. Pitzer, *J. Chem. Phys.* **92**, 3096 (1990); see also D. R. Schreiber and K. S. Pitzer, *Fluid Phase Equilib.* **46**, 113 (1989).

- ¹¹³J. Dudowicz, K. F. Freed, and J. F. Douglas, Phys. Rev. Lett. **92**, 045502 (2004).
- ¹¹⁴H. W. Xiang, Fluid Phase Equilib. **187–188**, 221 (2001); H. W. Xiang, Int. J. Thermophys. **22**, 919 (2001).
- ¹¹⁵S. V. Kazakov and N. I. Chernova, Russ. J. Phys. Chem. **69**, 1010 (1995); P. D. Macedo and J. S. Simmons, J. Res. Natl. Bur. Stand., Sect. A **78A**, 53 (1974).
- ¹¹⁶K. S. Pitzer, J. Phys. Chem. **99**, 13070 (1995).
- ¹¹⁷J. Xu and D. R. Herschbach, J. Phys. Chem. **96**, 2307 (1992); D. Ben-Amotz and D. R. Herschbach, Isr. J. Chem. **30**, 59 (1990).
- ¹¹⁸E. M. Holleran, J. Phys. Chem. **72**, 1230 (1969); **73**, 167 (1969); J. Chem. Phys. **49**, 39 (1968).
- ¹¹⁹C. Vega, C. McBride, and C. Menguina, Phys. Chem. Chem. Phys. **4**, 3000 (2002).
- ¹²⁰G. A. Inglesias-Silva and K. R. Hall, Ind. Eng. Chem. Res. **40**, 1948 (2001).